3. Latest Cretaceous–Earliest Oligocene and Quaternary Dinoflagellate Cysts, ODP Site 1172, East Tasman Plateau[1]

H. Brinkhuis,[2] S. Sengers,[2] A. Sluijs,[2] J. Warnaar,[2] and G.L. Williams[3]

ABSTRACT

Palynomorphs were studied in samples from Ocean Drilling Program (ODP) Leg 189, Holes 1172A and 1172D (East Tasman Plateau; 2620 m water depth). Besides organic walled dinoflagellate cysts (dinocysts), broad categories of other palynomorphs were quantified in terms of relative abundance. In this contribution, we provide an overview of the dinocyst distribution from the Maastrichtian to lowermost Oligocene and Quaternary intervals and illustrate main trends in palynomorph distribution. The uppermost Cretaceous–lowermost Oligocene succession of Site 1172 has a confident biomagnetostratigraphy, enabling us to tie early Paleogene Southern Hemisphere dinocyst events to the geomagnetic polarity timescale for the first time.

Dinocyst species from the Maastrichtian to earliest Oligocene at Site 1172 are largely endemic ("Transantarctic Flora") or bipolar; cosmopolitan taxa are present in the background as well. The Maastrichtian–early late Eocene dinocyst assemblages are indicative of shallow-marine to restricted marine, pro-deltaic conditions, closely tied to a massive siliciclastic sequence. By middle late Eocene times (~35.5 Ma), the siliciclastic sequence gave way to a thin glauconitic unit, considered to reflect the deepening of the Tasmanian Gateway. This transition coincides with the most prominent change in dinocyst associations of the Paleogene. The turnover is inferred to reflect a change from marginal marine to more offshore conditions, with increased winnowing and ox-

idation. Overlying pelagic carbonate ooze of middle early Oligocene and younger age is virtually barren of organic microfossils, although Quaternary assemblages have been recovered. This aspect is taken to reflect average low sedimentation rates and well-oxygenated water masses during most of the Oligocene and Neogene. The few palynologically productive samples from the Oligocene–Quaternary interval have a stronger cosmopolitan to subtropical signature, with warm-water species being common to abundant.

INTRODUCTION

Ocean Drilling Program (ODP) Site 1172 is located in a water depth of ~2620 m on the flat western side of the East Tasman Plateau (ETP), ~170 km southeast of Tasmania (Fig. F1). At 44°S, the site lies in cool subtropical waters just north of the Subtropical Front. During the middle Eocene, however, the ETP was at ~65°S when its relatively fast northward movement (55 km/m.y.) with Australia commenced (Shipboard Scientific Party, 2001a). Drilling at Site 1172 penetrated some 766 m of uppermost Cretaceous–Quaternary sediments. Initial studies indicated that ~70 m of black shallow-marine mudstones of latest Cretaceous (Maastrichtian) age are overlain by ~335 m of Paleocene and Eocene brown, green, and gray shallow-marine mudstones and ~364 m of Oligocene and Neogene pelagic carbonates (Shipboard Scientific Party, 2001c). The pelagic carbonates reflect ever-increasing depths following relatively rapid latest Eocene–earliest Oligocene subsidence, while much of the Oligocene and lower Miocene section is thought to be missing because of current action. Underlying Paleogene and latest Cretaceous siliciclastics were deposited at shallow depths. The sedimentary record at Site 1172 thus has captured the tectonic evolution of the opening of the Tasmanian Seaway, its deepening, and the voyage northward from ~70°S to its present location at 44°S.

Shipboard palynological analysis indicated that well-preserved organic walled dinoflagellate cysts (dinocysts) and sporomorphs are present in the Quaternary interval. In contrast, it appeared that the remaining Neogene–lower Oligocene strata are virtually devoid of acid-resistant organic matter, whereas dinocysts are the dominant constituent of the rich Maastrichtian to earliest Oligocene palynological associations. Other microfossils are present in the Cenozoic and uppermost Cretaceous sequence at Site 1172 with the dominance of different groups changing with depositional environments. Calcareous groups are most prominent from the Oligocene upward, whereas siliceous and organic groups are most common below this level (see overview in Shipboard Scientific Party, 2001c). The basic architecture of the sedimentary succession of Site 1172 is similar to that of the other Leg 189 sites in recording three major phases of paleoenvironmental development, namely (1) Maastrichtian–early late Eocene deposition of shallow-water siliciclastic sediments during rifting between Antarctica and the South Tasman Rise (STR), (2) a transitional latest Eocene condensed interval with shallow-water glauconitic siliciclastic sediments giving way to deepwater pelagic carbonates representing the activation of bottom currents as the Tasmanian Gateway deepened during early drifting, and (3) earliest Oligocene–Quaternary deposition of pelagic carbonate sediments in increasingly deeper waters and more open-ocean conditions as the Southern Ocean developed and expanded with the north-

F1. Leg 189 drilling locations, p. 22.
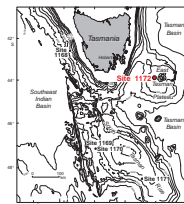
ward flight of the ETP and the Australian continent (Shipboard Scientific Party, 2001a).

The primary objectives of coring and logging at Site 1172 were to:

1. Obtain an Oligocene–Holocene pelagic carbonate section to construct moderate to high-resolution paleoceanographic and biostratigraphic records,
2. Obtain an Eocene siliciclastic sediment sequence for better understanding of paleoceanographic and paleoclimatic conditions before Antarctic Circumpolar Current development,
3. Obtain an Eocene–Oligocene transitional sequence to determine the effects of the initial opening of the Tasmanian Gateway on the paleoceanography of the Pacific Tasmanian margin, and
4. Compare and contrast changing paleoenvironmental and paleoceanographic conditions on each side of Tasmania (Site 1168) as the Tasmanian Seaway opened and the Antarctic Circumpolar Current developed (Shipboard Scientific Party, 2001c).

For this purpose, a selection of samples from Holes 1172A and 1172D, covering the Maastrichtian–lowermost Oligocene, was palynologically analyzed. In addition, a selection of samples from the Quaternary interval was analyzed as well. Considering that the latest Cretaceous–Paleogene succession of Site 1172 has a confident magnetostratigraphy, calibrated against biotic events, great potential to tie dinocyst events to the geomagnetic polarity timescale (GPTS) and cyclostratigraphy (Röhl et al., submitted [N1]) is available here.

Shipboard analysis indicated that most of the Oligocene–Pliocene interval is barren of organic remains, and follow-up studies thus far have not further considered this interval. However, since these findings are only based on core catcher materials and onboard processing, further study should confirm this aspect. Here, we provide an overview of the dinocyst distribution from the Maastrichtian to lowermost Oligocene and Quaternary interval. Several new taxa have been recorded; some of them are informally characterized herein and others are placed in broad generic groups. Future work on this material will describe these taxa formally, and more details, also on other constituents of applied generic groupings, will be presented. Results of more detailed studies, including palynology, considering prominent boundaries at Site 1172 (e.g., Eocene/Oligocene, Paleocene/Eocene, and Cretaceous/Tertiary boundaries) are presented elsewhere (Sluijs et al., this volume; Stickley et al., submitted [N2]; Röhl et al., submitted [N1], [N3]; Schellenberg et al., submitted [N4]).

MATERIAL AND METHODS

Hole 1172A was piston cored to 522.6 meters below sea floor (mbsf) with 92.6% recovery. Hole 1172D was rotary cored from 344 to 373 mbsf, washed to 497 mbsf, and rotary cored to 766 mbsf with 80% recovery. Hole 1172D penetrated ~70 m of black shallow-marine mudstones of latest Cretaceous (Maastrichtian) age (to 766 mbsf). This sequence is overlain by ~335 m of Paleocene and Eocene brown, green, and gray shallow-marine mudstones, partly recovered in Hole 1172D (from 497 to 766 msbf) and down (and partly overlapping) to 522 mbsf in Hole 1172A. The lithostratigraphic sequence has been divided into four units, with three subunits in Unit I and two subunits in Units III

and IV. For details, see the Leg 189 *Initial Reports* volume (Exon, Kennett, Malone, et al., 2001; Shipboard Scientific Party, 2001a, 2001b). The most remarkable lithologic change occurs at ~360 mbsf, within lithostratigraphic Unit II. This unit (355.8–361.12 mbsf) is a relatively thin uppermost Eocene–Oligocene (E-O) transitional unit. The sediments are mainly characterized by increased glauconite content and consist of variations of greenish gray glauconite-bearing silty diatomaceous claystone and dark greenish gray glauconitic diatomaceous clayey siltstone. This transition was considered to represent a condensed section or a hiatus. Carbonate content decreases from 69 wt% at the top to 0.3 wt% at the base (Shipboard Scientific Party, 2001c). Postcruise studies indicated the Cretaceous/Tertiary boundary (KTB) occurs at ~696 mbsf, marked by a distinct hardground. At this level, homogenous black mud to siltstones change over into more glauconite-rich gray to black sand and siltstones (see review in Shipboard Scientific Party, 2001c).

Reconstructed sedimentation rates at Site 1172 represent three distinct phases. In contrast to other Leg 189 sites, sedimentation rates were relatively low (between 2.6 and 1.04 cm/k.y.) in the Maastrichtian–uppermost Eocene. From the uppermost Eocene–middle Miocene (15 Ma), sedimentation rates decreased (0.16–3.2 cm/k.y.) and increased thereafter until the present day (see "Age Model," p. 5). These three basic intervals coincide with the succession in global climate change from the so-called "Greenhouse," via "Doubthouse," to "Icehouse" states. Site 1172, like Site 1168, appears to have been strategically located to record these overall shifts in global climate associated with development of the Antarctic cryosphere (Shipboard Scientific Party, 2001a). The most conspicuous change in the sediment and biotic sequence occurred during the transition from the latest Eocene to the earliest Oligocene, with conspicuous reduction in sedimentation rates and deposition of glauconite sands. Like at other Leg 189 sites, this transition reflects a transient event associated with temporarily increased bottom water activity in the basin. The timing of this episode is consistent with the hypothesis linking the deepening of the Tasmanian Gateway, major cooling of Antarctica, and associated cryospheric development (see also Stickley et al., submitted [N2]). However, these links are—as yet—poorly understood (see discussion in Huber et al., submitted [N5]). Moreover, the Oligocene–Quaternary sedimentary succession at Site 1172 was also interpreted to reflect an increase in ventilation (i.e., leading to a, at best, patchy Neogene palynological record). Like the other sites drilled during Leg 189, increased ventilation resulted from a fundamental change in paleogeography and oceanic circulation associated with increasing dispersal of the southern continents and the opening and/or deepening of the ocean basins at high latitudes in the Southern Hemisphere. For further information on the general geologic and oceanographic setting of Site 1172, see Shipboard Scientific Party (2001c).

On average, two to three samples per core (average spacing = ~3–4 m) from Holes 1172A and 1172D were palynologically analyzed (Tables **T1, T2, T3**). In certain intervals (Quaternary, Eocene/Oligocene, and Cretaceous/Tertiary), samples are more closely spaced (Tables **T1, T2, T3**). Results from onboard studies using core catcher samples have been integrated here with this first follow-up study.

T1. Quaternary palynological results, Hole 1172A, p. 24.

T2. Eocene–Oligocene palynological results, Hole 1172A, p. 26.

T3. Maastrichtian–Eocene palynological results, Hole 1172D, p. 27.

Palynological Processing and Counting

Organic walled microfossils were extracted for analysis using standard palynological processing techniques at the Palynological Laboratory at the University of Utrecht.

From the core samples, ~15 g of wet sediment was collected, oven dried at 60°C, and weighed (8–14 g). Processing involved an initial treatment in hydrochloric acid (10%) to dissolve carbonates, followed by a treatment of hydrofluoric acid (38%) to dissolve silicates. After each acid step, samples were washed two times by decanting after 24 hr settling and filling up with water. The hydrofluoric step included 2 hr shaking at ~250 rpm and adding 30% hydrochloric acid to remove fluoride gels. Then, samples were repeatedly washed in distilled water and finally sieved through a 15-µm nylon mesh sieve (10–µm nylon mesh sieve for Quaternary samples). To break up clumps of residue, the sample was placed in an ultrasonic bath for a maximum of 5 min after the first sieving. The residue remaining on the sieve was transferred to a glass tube. The tubes were centrifuged for 5 min at 2000 rpm and the excess amount of water was removed. For slide preparation, residues were transferred to vials and glycerin water was added. The residue was homogenized, no coloring was added, a droplet of each residue was mounted on a slide with glycerin jelly, and the mixture was stirred and sealed with nail varnish. Two to four slides per sample were prepared.

Where possible, slides were initially counted to up to 200 or more dinocysts, while also counting associated other palynomorphs. When dealing with low yields of dinocysts, counting was stopped after two slides were examined (see Tables T1, T2, T3). Dinocysts were counted at species level, while other palynomorphs were counted in broad categories (namely, bisaccate pollen, other pollen spores, spores, inner linings of foraminifers [if more than three chambers], prasinophyte algae like *Cymatiosphaera* and *Tasmanite*s spp., remains of Copepod eggs, and acritarchs).

The postcruise studies are here supplemented by the onboard studies performed on core catcher material. Essentially, shipboard processing followed the steps as described above but used a 20-µm stainless steel sieve (i.e., leading to the potential loss of small palynomorphs) and equipment was not as sophisticated as common modern laboratory setups. Results from these shipboard samples should be taken as rough estimations.

Cyst taxonomy follows that cited in Williams et al. (1998) and Rochon et al. (1999). A species list, including remarks on new taxa, is presented in the "Appendix," p. 17. For the purpose of the present study, only providing an overview of the dinocyst distribution and general palynological contents, emphasis is placed on potential age-diagnostic taxa. Other species are placed in generic groups (see Tables T1, T2, T3). Future studies will consider dinocyst distribution of rare species, and so on, besides other aspects, in more detail.

Age Model

We adopt the postcruise age model as presented in Stickley et al. (this volume) for Holes 1172A and 1172D. Ages (in Ma) are indicated in Tables T1, T2, T3, and T4 and in Figure F2 where relevant; for more detailed information see Stickley et al. (this volume). As an indication, the Pliocene/Pleistocene boundary occurs at ~21 mbsf, the early/late Pliocene boundary at ~49 mbsf, the Miocene/Pliocene boundary at ~87

T4. Age-indicative dinocyst events, Holes 1172A–1172D, p. 28.

F2. Terrestrial palynomorphs and offshore dinocysts, p. 23.
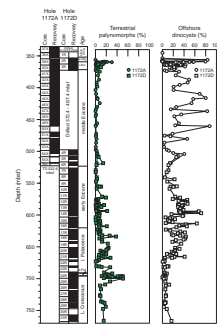
mbsf, the middle/late Miocene boundary at ~238 mbsf, the early/middle Miocene boundary at ~311 mbsf, the Oligocene/Miocene boundary at ~335 mbsf, the early/late Oligocene boundary at ~354 mbsf, the Eocene/Oligocene boundary (sensu Global Stratotype Section and Point; GSSP) at ~356 mbsf, the middle/late Eocene boundary at ~377 mbsf, the early/middle Eocene boundary at ~550 mbsf, the Paleocene/Eocene boundary at ~620 mbsf, the middle/late Paleocene boundary at ~692 mbsf, and the KTB at ~696 mbsf. The bottom of Hole 1172D at 766 mbsf represents the earliest Maastrichtian.

RESULTS AND DISCUSSION

Palynomorph and dinocyst distribution, as well as percentages of off-shore (oceanic) dinocysts and terrestrial palynomorphs (see explanation below), are depicted in Tables T1, T2, T3. A summary of selected stratigraphically useful dinocyst events and derived ages is given in Table T4. Plots of percent terrestrial palynomorphs and percent offshore dinocysts vs. depth and age are given in Figure F2. Illustrations of taxa are shown in Plate P1.

Palynology: General

Dinocysts are in most cases the most prominent palynomorphs throughout. Sporomorphs may dominate the Maastrichtian part of the succession and are frequent in the overlying palynological associations, notably in the upper Paleocene and lower Eocene (Fig. F2). Skolochorate acritarchs of various types, as well as remains of chlorophyte algae and foraminifer inner linings, occur in the background in the Paleogene and Quaternary associations (Tables T1, T2, T3).

Dinoflagellate Cysts: General

Although many attempts to study Oligocene–Neogene dinocysts in the circum-Antarctic domain have been undertaken, they have only sporadically been found. Apparently, too often the organic wall of the dinocyst is not resistant to the oxygen-rich waters in the Antarctic domain and/or winnowing at depth, and low sedimentation rates preclude preservation of these microfossils (see discussion in Brinkhuis et al., this volume). Nevertheless, progress over the recent years has resulted in the documentation of an Antarctic Oligocene–earliest Miocene assemblage from the Ross Sea continental shelf (Cape Roberts Project; CRP) and several Miocene–Quaternary assemblages from the Weddell and Scotian Seas. (e.g., Wrenn et al., 1998; Hannah et al., 1998, 2000; McMinn et al., 2001; Harland and Pudsey, 1999, 2002; Harland et al., 1998, 1999).

In contrast, Late Cretaceous and Paleogene dinocysts from the broad Antarctic Realm or Southern Ocean are comparatively well known, notably from southern South America and from the James Ross and Seymour Islands, but also from southeastern Australia, New Zealand, from erratics along the Antarctic margin, the Ross Sea continental shelf (CRP), besides from several ocean drill sites (see overviews in, e.g., Haskell and Wilson, 1975; Askin, 1988a, 1988b; Wilson, 1985, 1988; Wrenn and Hart, 1988; papers in Duane et al., 1992; Pirrie et al., 1992; Mao and Mohr, 1995; Truswell, 1997; Hannah, 1997, Hannah et al., 2000; Levy and Harwood, 2000; Guerstein et al., 2002; Brinkhuis et al.,

P1. Illustrations of taxa, p. 30.
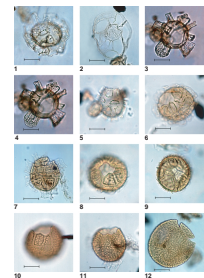
this volume). Therefore, many studies have documented Circum-Antarctic/Southern Ocean Upper Cretaceous and Paleogene dinocyst distribution and taxonomy in great detail. Typically, however, meaningful chronostratigraphic calibration of dinocyst events is a classic problem due to the general absence of other age-indicative biota and/or magnetostratigraphy or other means of dating when dinocysts are encountered. Only recently, for the first time, integrated Oligocene–lowermost Miocene biomagnetostratigraphy, including dinocysts, was achieved on the basis of successions drilled during the Cape Roberts Project (Hannah et al., 1998, 2000).

Dinocyst species in the Maastrichtian–uppermost Eocene at Site 1172 are largely endemic (the so-called "Transantarctic Flora" sensu Wrenn and Beckmann, 1982) or bipolar; cosmopolitan taxa are present in varying, but on average, lower abundance as well. The lowermost Oligocene (a single productive sample only) and Quaternary interval has a stronger cosmopolitan to subtropical signature, with typical temperate to warm-water taxa being common to abundant, discussed further below.

The lower Paleogene dinocyst stratigraphic succession as well as its broad age range matches that known from New Zealand (e.g., Wilson, 1988, and references therein; Crouch, 2001). Maastrichtian–Paleocene associations are virtually identical to those known from Seymour Island (e.g., Askin, 1988a, 1988b; Elliot et al., 1994) and New Zealand (e.g., Wilson, 1978, 1984; Willumsen, 2000). During the middle Eocene, influence of the transantarctic dinocyst flora, constituted by species like *Deflandrea antarctica, Octodinium askiniae, Enneadocysta partridgei, Vozzhennikovia* spp., *Spinidinium macmurdoense,* and so on, increases and continues until the middle late Eocene. This aspect is quite different from the distribution patterns recorded at Site 1168 (**Brinkhuis et al.,** this volume). The E-O transition is marked by a turnover from transantarctic dominated to associations dominated by new species of *Brigantedinium* and *Deflandrea* and the influx of *Stoveracysta kakanuiensis*. Lower Oligocene deposits are barren of palynomorphs, except for a single productive sample.

Several new taxa are recorded (e.g., new species of *Batiacasphaera, Cerebrocysta, Cerodinium, Enneadocysta, Operculodinium, Dinopterygium, Impagidinium, Spiniferites, Vozzhennikovia*, and *Spinidinium*), which will be treated in more detail elsewhere (see also "Appendix," p. 17).

Maastrichtian

The Maastrichtian interval is characterized by relative abundant *Manumiella* spp., a typical situation for Antarctic dinocyst associations at this time (e.g., Wilson, 1978, 1984; Askin, 1988a, 1988b, 1999; Smith, 1992; Willumsen, 2000). No effort is taken here to further subdivide this group, but morphotypes (species) like *Manumiella druggii, Manumiella seelandica,* and *Manumiella seymourensis* are present, with the first being the most common. *Alterbidinium* (notably *Alterbidinium acutulum), Diconodinium, Palaeocystodinium*, and *Cerodinium* spp. further represent peridinioid cysts, including several new species. In general, peridinioid species (probably heterotrophic) are far more abundant than gonyaulacoid (autotrophic) cysts. In addition, new species of *Operculodinium, Dinopterygium*, and *Spiniferites* are prominent in these associations (Table T3). Of stratigraphic importance are the last occurrence (LO) of *Odontochitina operculata* near the base of the succession and the first occurrence (FO) of the *Alisocysta reticulata* group and *Alisocysta circumtabulata*, confirming a Maastrichtian age (cf. Askin, 1988a, 1988b;

Willumsen, 2000). The KTB is here (at 696 mbsf in Hole 1172D), marked by the demise of *Manumiella* spp. and the massive influx of *Palaeoperidinium pyrophorum,* a feature also known from Seymour Island and New Zealand KTB successions (Askin, 1988a, 1988b; Willumsen, 2000). In the background, typical earliest Danian indicators like *Trithyrodinium evittii* and *Senoniasphaera inornata* have their FO (cf., e.g., Wilson, 1984; Strong et al., 1995; Brinkhuis et al., 1998). The massive turnover in the dinocyst assemblages, in conjunction with the recognized hardground at ~696 mbsf (near the top of Section 189-1172D-24R-5) point to a hiatus at the KTB. Occurrences of early Danian taxa (i.e., *Trithyrodinium evittii* and *Senoniasphaera inornata*) below the hardground are considered to result from downward bioturbation. The KTB hiatus apparently spans Chron C29R (**Stickley et al.,** this volume; Schellenberg et al., submitted [**N4**]).

Paleocene

The Paleocene interval is marked by overall low-diversity, high-dominance episodes, (like, e.g., an acme of *Glaphyrocysta* spp.). In general, low-diversity associations prevail, with *Cerodinium, Palaeocystodinium, Operculodinium, Hystrichosphaeridium,* and *Spiniferites* spp. being common. Representatives of *Alisocysta*, *Pyxidinopsis,* and *Alterbidinium* consistently occur in the background. *Palaeoperidinium pyrophorum*, abundant just above the KTB (in Section 189-1172D-24R-5), is virtually absent in samples from Core 189-1172D-23R and younger. This species has a global LO near the base of the upper Paleocene (Thanetian) (e.g., Powell et al., 1995; Crouch, 2001; **Williams et al.,** this volume), and this and other selected events (Table **T4**) suggest a late Paleocene age for the sequence until ~620 mbsf. This is confirmed by the FO of *Deflandrea* spp. near the top of this interval (cf. Crouch, 2001). Most of the lower and middle Paleocene (Danian–Seelandian) appears therefore to be missing or is extremely condensed.

Globally, the top of the Paleocene is marked by a massive influx of *Apectodinium* spp., especially during the Paleocene/Eocene Thermal Maximum or PETM (e.g., Bujak and Brinkhuis, 1998; Crouch et al., 2001; Crouch, 2001). The FO of representatives of the genus heralds this phase during the latter half of the Paleocene. Many zonation schemes, like that of Wilson (1988) from New Zealand, make use of this aspect for recognition of the late Paleocene. In relevant samples from Hole 1172D, representatives of *Apectodinium* are sparse at best and an acme is conspicuously absent. This suggests that the typical PETM succession has not been recovered at Site 1172, either due to a hiatus or to core recovery problems (bad luck). Alternatively, because *Apectodinium* represents a tropical genus, climatic conditions, despite the general warmth at the end of the Paleocene, may just not have allowed a significant manifestation at these paleolatitudes. The Paleocene/Eocene hiatus or core gap may be small, as discussed elsewhere (Röhl et al., submitted [**N3**]).

Early and Middle Eocene

The lower Eocene in essence forms a continuation of the upper Paleocene succession, with a relative abundance of species of *Deflandrea, Palaeocystodinium, Operculodinium, Hystrichosphaeridium,* and *Spiniferites*, besides typical early Eocene taxa like *Dracodinium waipawaense, Samlandia delicata* group, and the *Pyxidinopsis waipawaensis* group being con-

sistently present (cf. Crouch, 2001). Around the early–middle Eocene transition, important FOs include those of the *Charlesdowniea edwardsii* group, *Arachnodinium antarcticum, Membraniphoridium perforatum,* and *Hystrichokolpoma spinosum.* Of significant interregional importance is also the FO of *Enneadocysta* spp., including *Enneadocysta partridgei* and *Enneadocysta* sp. A, near the early/middle Eocene boundary. The succession of these events broadly matches those reported from the New Zealand region (e.g., Wilson, 1988; Hannah and Raine, 1997) from coeval deposits. The calibration against magnetostratigraphy as reached herein now allows more confident dating of early–middle Eocene deposits around Southern Ocean sites (see Table **T4**). However, some typical Eocene Southern Hemisphere taxa like *Arachnodinium antarcticum* and *Enneadocysta partridgei* have an LO at the early/late Oligocene boundary in this area according to Hannah and Raine (1997). Although this aspect is discussed further below (see **"Late Eocene–Earliest Oligocene"** below) and elsewhere (**Sluijs et al.,** this volume; Stickley et al., submitted [**N2**]), it may be noted here that these "young" LOs are here considered a result of reworking. *Arachnodinium antarcticum*, for example, has a consistent top associated with Subchron C18n1n, also at Sites 1170 and 1171 following shipboard studies and updated age models (**Stickley et al.,** this volume; Stickley et al., submitted [**N2**]; Röhl et al., submitted [**N1**]).

Although the late Paleocene and early Eocene associations already compose a large portion of typical endemic Antarctic taxa, endemism increases even more toward the end of the early Eocene. The early–middle Eocene transition is marked by a strong influx of endemic (Transantarctic) species like *Deflandrea antarctica, Octodinium askiniae, Enneadocysta partridgei,* and *Vozzhennikovia* spp. and/or bipolar (high latitude) taxa like *Spinidinium macmurdoense* and the *Phthanoperidinium echinatum* group (cf. Firth, 1996).

The younger part of the Southern Ocean middle Eocene is comparatively less well studied than the underlying part. Only few comparisons may be made to New Zealand (e.g., Wilson, 1988; Strong et al., 1995; Edbrooke et al., 1998; Hannah et al., 1997), Deep-Sea Drilling Project [DSDP] Sites 280 and 281 (Crouch and Hollis, 1996), Seymour Island (Wrenn and Hart, 1988), Scotia Sea (Mao and Mohr, 1995), and southern Argentinian successions (e.g., Guerstein et al., 2002, and references therein), indicating a broad similarity. The younger part of the Southern Ocean middle Eocene appears to be characterized by several important LOs, including those of *Membranophoridium perforatum, Hystrichosphaeridium truswelliae, Arachnodinium antarcticum, Hystrichokolpoma spinosum,* and *Hystricholkopoma truncatum* (cf. Wilson, 1988) (see Table **T4**).

Late Eocene–Earliest Oligocene

Early late Eocene dinocyst distribution forms a continuation of the middle Eocene pattern. Transantarctic species predominate, and final acmes of *Enneadocysta partidgei*, the *Deflandrea antarctica* group, and *Spinidinium macmurdoense* are recorded. Important FOs in this phase include those of *Schematophora speciosa, Aireiana verrucosa, Hemiplacophora semilunifera,* and *Stoveracysta ornata*. Toward the middle late Eocene, FOs of *Achomosphaera alcicornu, Reticulatosphaera actinocoronata,* and *Alterbidinium distinctum* and the LO of *Schematophora speciosa* appear important for interregional correlation. *Vozzhennikovia* spp. continues to be a common constituent of the associations. The LO of *Schematophora*

speciosa is very close to the LO of abundant *Deflandrea antarctica* group, and the latter horizon marks a significant change in the associations, including a brief barren interval. Here, on one hand cosmopolitan taxa like *Turbiosphaera filosa, Cleistosphaeridium* spp., and *Lingulodinium machaerophorum* become prominent, whereas on the other hand, new species like *Deflandrea* sp. A and *Brigantedinium*? sp. dominate the succession. In addition, the FO of *Stoveracysta kakanuiensis* is recorded. Slightly upsection, in a succession dated by other means as approximately the E/O boundary (sensu GSSP), sediments become barren of organic microfossils to only briefly reappear in the early Oligocene (assigned to Chron C10) (Table T4). In this single productive sample thus far from the Oligocene, virtually all transantarctic Paleogene dinocysts have disappeared (only a single, poorly preserved, probably reworked specimen of *Enneadocysta partridgei* is recovered). The association in this sample (189-1172A-39X-2, 3–5 cm; 356.13 mbsf) is characterized by the abundance of taxa more typical for Tethyan waters, including an occurrence of *Hystrichokolpoma* sp. cf. *Homotryblium oceanicum* (e.g., Brinkhuis and Biffi, 1993; Wilpshaar et al., 1996; Brinkhuis et al., this volume [Site 1168]).

Some of the late Eocene dinocyst events have previously been reported from the Browns Creek section (Cookson and Eisenack, 1965; Stover, 1975). For example, the ranges of *Schematophora speciosa, Aireiana verrucosa, Hemiplacophora semilunifera,* and *Stoveracysta ornata* appear useful for regional and even global correlation. Many of the Browns Creek late Eocene dinocysts have been recorded from locations around the world, also in otherwise well-calibrated sections in central and northern Italy, including the Priabonian Type (Brinkhuis and Biffi, 1993; Brinkhuis, 1994). It appears that these index species have slightly earlier tops in this region than they have in Italy (Tethyan Ocean), if the records of Cookson and Eisenack (1965) and Stover (1975) are combined with more recent nannoplankton and magnetostratigraphic studies from the same section (Shafik and Idnurm, 1997). This aspect may be related to the progressive global cooling during the latest Eocene.

The upper Eocene succession at Site 1172 thus comprises the most prominent change in dinocyst associations of the Paleogene, pointing to important environmental changes influencing the site at this time. A similar transition is, albeit in less detail, reported by shipboard palynological analysis from Sites 1170 and 1171. More details on the E-O transition, also from other Leg 189 sites, and paleogeographic and oceanographic implications are presented and discussed presented in Sluijs et al. (this volume), in Stickley et al. (submitted [N2]), and in Huber et al. (submitted [N5]).

Quaternary

The Quaternary record throughout has reasonable palynological recovery (Table T3), whereas the underlying Oligocene–Pliocene interval is apparently barren, an aspect that may be related to changing oceanographic and depositional setting. Possibly, the stronger influence of the relatively warm (oxygen depleted) East Australian Current waters or productivity changes and/or less active bottom currents are involved in this aspect. The associations are typically dominated by oceanic dinocysts like *Nematosphaeropsis* and *Impagidinium* spp. (notably *Impagidinium aculeatum*, *Impagidinium paradoxum*, and *Impagidinium patulum*). Protoperidinioid species like *Brigantedinium* spp. are common in some samples. Occasionally, the cold-water species *Impagidinium pallidum* is

present as well. The overall distribution is very similar to that recorded in the Quaternary interval at Site 1168 (**Brinkhuis et al.,** this volume). These results indicate potential for future paleoceanographic studies involving dinocysts.

Paleoenvironmental Considerations

Clearly, the present results indicate potential for the application of quantitative palynological (dinocyst) analysis for climatic and environmental reconstructions (except for the upper Oligocene to Pliocene interval). Here, we are principally concerned with providing the overall trends. For this purpose, trends in the relative abundance of terrestrial palynomorphs and offshore (oceanic) dinocysts are depicted in Figure **F2.** Species marked with (o) in Tables **T2** and **T3** have been used to generate this curve, making use of previous studies focusing on modern dinocyst distribution (e.g., Rochon et al., 1999) and empirical paleoenvironmental evidence from a wide variety of sources (see, e.g., overviews in Brinkhuis and Biffi, 1993; Brinkhuis, 1994; Stover et al., 1996), including the shipboard study on the middle middle Eocene of Site 1170 (Shipboard Scientific Party, 2001b). In that study, it is shown that *Enneadocysta* maxima correlate with calcareous nannoplankton optima. *Enneadocysta* is therefore included in the offshore dinocyst category, seen to reflect relatively oligotrophic, offshore settings.

The upper Maastrichtian–lower upper Eocene succession at Site 1172 was interpreted to reflect relatively warm climatic conditions and very shallow water to restricted marine conditions with marked runoff (Shipboard Scientific Party, 2001a, 2001b). The absence of planktonic foraminifers, and even of calcareous nannofossils, in most parts of the Paleocene–middle Eocene confirms the envisaged overall marginal marine nature of the deposits. Older Maastrichtian sediments were deposited in more open-marine conditions based on higher abundances of calcareous microfossils, more offshore dinocyst assemblages, and few pyritized diatoms. The results of the present study further confirm this interpretation (Fig. **F2**). Similar reconstructions were proposed for the overall similar KTB successions at Seymour Island (Askin, 1988a, 1988b; 1999). Future studies may reveal more detail, for example, concerning sea level change and the nature of the recorded Milankovitch cyclicities (Röhl et al., submitted [**N1**]).

The upper middle Eocene is marked by a rather gradual change from an inner neritic setting to more offshore conditions. High sporomorph influx and low-diversity/high-dominance dinocyst assemblages with prominent *Deflandrea* spp., indicating marked freshwater influence and corresponding eutrophic conditions and, possibly, sluggish circulation, characterize the older Eocene deposits. These evolve into more offshore, deeper marine environments with increased ventilation and bottom water current activity, with prominent *Enneadocysta* spp. (see also Shipboard Scientific Party, 2001c, and Röhl et al., submitted [**N1**]). The increased numbers of endemic Antarctic dinocyst species in this phase may indicate concomitant cooling and/or isolation of water masses, whereas warmer episodes may also be recognized. The E-O transition (35.5–33.3 Ma) is marked by a series of distinct stepwise environmental changes, seen to reflect cooling and coeval rapid deepening of the basin (**Sluijs et al.,** this volume; Stickley et al., submitted [**N2**]). Combined evidence indicates increasing bottom water ventilation and the appearance of highly productive offshore surface waters in outer neritic to bathyal depositional settings associated with the deepening of the Tas-

manian Gateway (Stickley et al., submitted [N2]). This trend culminated in the early Oligocene (33–30 Ma) when rigorous ventilation and/or oxygen-rich bottom waters precluded sedimentation of organic matter, despite overall high surface water productivity. The condensed pelagic calcareous sequence contains abundant siliceous microfossils and was deposited in an oceanic bathyal environment. Oligocene to present-day pelagic carbonates were deposited in well-ventilated open-ocean conditions.

The curves of Figure F2 both confirm the broad trend of initial shallow-marine, near continental conditions, evolving into an open oceanic environment. Variations in both curves during the Maastrichtian–early Oligocene may be explained by the influence of eustatic sea level changes, as further research will possibly show in more detail (see also Röhl et al., submitted [N1]). A marginal marine, pro-deltaic setting during the Maastrichtian–middle Eocene matches the low-diversity dinocyst assemblages, with cyclic optima of peridinioid species like *Alterbidinium, Cerodinium, Deflandrea, Phthanoperidinium, Spinidinium,* and *Vozzhennikovia* spp. and gonyaulacoid taxa such as *Enneadocysta, Operculodinium,* and *Spiniferites* spp. The dinocyst assemblages in this part of the core are very similar to those recorded elsewhere from ancient pro-delta deposits (Brinkhuis et al., 1992; Brinkhuis, 1994). The middle and late Eocene are characterized by a slight increase in diversity, with more consistent occurrences of open-marine, neritic to offshore taxa like *Enneadocysta* spp., *Thalassiphora pelagica, Cleistosphaeridium,* and *Hystrichokolpoma* spp., besides increasing numbers of typical oceanic taxa like *Nematosphaeropsis* and *Impagidinium* spp. (cf. Fig. F2) (see also Röhl et al., submitted [N1]).

A general eutrophic nature of the surface waters influencing Site 1172 during the Paleogene is suggested from the high abundance of peridinioid, presumably heterotrophic, species (cf. Brinkhuis et al., 1992). This general pattern matches an initial pro-deltaic setting, changing into a more open-oceanic eutrophic (upwelling?) setting (see for further discussion Sluijs et al., this volume, and Stickley et al., submitted [N2]).

CONCLUDING REMARKS

Central to the mission of Leg 189 was (and is) to analyze the Eocene siliciclastic sediment sequence for better understanding of paleoceanographic and paleoclimatic conditions before Antarctic Circumpolar Current development and to determine the timing and the effects of the deepening of the Tasmanian Gateway and presumably related Antarctic Circumpolar Current development on the paleoceanography of the Pacific Tasmanian margin. Clearly, our results indicate great potential for the application of quantitative palynological analysis for these stratigraphic, climatic, and environmental reconstructions (except perhaps for the upper Oligocene–Pliocene interval) using materials from Site 1172. Further study, involving higher-resolution analysis is presented in follow-up contributions, notably on nature of the KTB, PETM, and E-O transition (e.g., Sluijs et al., this volume; Stickley et al., submitted [N2]; Röhl et al., submitted [N1], [N3]; Schellenberg et al., submitted [N4]). A compilation of Site 1172 stratigraphically important dinocyst events and comparisons with global dinocyst stratigraphic distribution is provided in Williams et al. (this volume).

Comparison between results from Site 1172 and other Leg 189 sites with previous circum-Antarctic dinocyst studies, including the recent

CRP results, reveals that early Paleogene assemblages are throughout comparable, with the exception of the south coast of Australia—offshore eastern Tasmania (Site 1168) (**Brinkhuis et al.,** this volume; Huber et al., submitted [**N5**]). It follows that surface water conditions (i.e., paleoceanographic and climatological conditions) must have been roughly similar throughout the circum-Antarctic region at this time. This aspect drastically changes across the E/O boundary. The—albeit in a single sample—recovered earliest Oligocene dinocyst assemblage of Site 1172 has a distinct warm-temperate cosmopolitan character, whereas coeval assemblages immediately to the south remain endemic Antarctic or bipolar in nature (Hannah et al., 2000; CRP results). Meanwhile, endemic Antarctic Paleogene dinocysts are virtually absent at Site 1168 (**Brinkhuis et al.,** this volume). Considering that dinocysts should strongly reflect surface water conditions, a complex evolution of the Southern Ocean oceanographic circulation pattern across the E/O boundary thus emerges from our study. Comparison with results from other (micro) fossil groups and the resulting paleoceanographic implications, including possible relationships between the deepening of the Tasmanian Gateway, circulation changes, and initial Antarctic cryospheric development, is considered outside the scope of this study, but are presented and discussed elsewhere (Stickley et al., submitted [**N2**]; Huber et al., submitted [**N5**]).

ACKNOWLEDGMENTS

REFERENCES

Askin, R.A., 1988a. Campanian to Paleocene palynological succession of Seymour and adjacent islands, northeastern Antarctic Peninsula. *In* Feldmann, R.M., and Woodburne, M.O. (Eds.), *Geology and Paleontology of Seymour Island, Antarctic Peninsula.* Mem.—Geol. Soc. Am., 169:131–153.

————, 1988b. The palynological record across the Cretaceous/Tertiary transition on Seymour Island, Antarctica. *In* Feldmann, R.M., and Woodburne, M.O. (Eds.), *Geology and Paleontology of Seymour Island, Antarctic Peninsula.* Mem.—Geol. Soc. Am., 169:155–162.

————, 1999. *Manumiella seymourensis* new species, a stratigraphically significant dinoflagellate cyst from the Maastrichtian of Seymour Island, Antarctica. *J. Paleontol.,* 73:373–379.

Brinkhuis, H., 1994. Late Eocene to early Oligocene dinoflagellate cysts from the Priabonian type-area (Northeast Italy): biostratigraphy and paleoenvironmental interpretation. *Palaeogeogr., Palaeoclimatol., Palaeoecol.,* 107:121–163.

Brinkhuis, H., and Biffi, U., 1993. Dinoflagellate cyst stratigraphy of the Eocene/Oligocene transition in central Italy. *Mar. Micropaleontol.,* 22:131–183.

Brinkhuis, H., Bujak, J.P., Smit, J., Versteegh, G.J.M., and Visscher, H., 1998. Dinoflagellate-based sea surface temperature reconstructions across the Cretaceous-Tertiary boundary. *Palaeogeogr., Palaeoclimatol., Palaeoecol.,* 141:67–83.

Brinkhuis, H., Powell, A.J., and Zevenboom, D., 1992. High-resolution dinoflagellate cyst stratigraphy of the Oligocene/Miocene transition interval in Northwest and central Italy. *In* Head, M.J., and Wrenn, J.H. (Eds.), *Neogene and Quaternary Dinoflagellate Cysts and Acritarchs:* Salt Lake City (Publishers Press), 219–258.

Bujak, J.P., and Brinkhuis, H., 1998. Global warming and dinocyst changes across the Paleocene/Eocene boundary. *In* Aubry, M.-P., et al. (Eds.), *Late Paleocene-Early Eocene Climatic and Biotic Events in the Marine and Terrestrial Records:* New York (Columbia Univ. Press), 277–295.

Cookson, I.C., and Eisenack, A., 1965. Microplankton from the Browns Creek clays, SW Victoria. *Proc. R. Soc. Victoria,* 79:119–131.

Crouch, E.M., 2001. Environmental change at the Paleocene–Eocene biotic turnover [Ph.D. thesis]. Utrecht University, Utrecht, The Netherlands.

Crouch, E.M., Heilmann-Clausen, C., Brinkhuis, H., Morgans, H.E.G., Rogers, K.M., Egger, H., and Schmitz, B., 2001. Global dinoflagellate event associated with the Late Paleocene Thermal Maximum. *Geology,* 29:315–318.

Crouch, E.M., and Hollis, C.J., 1996. Paleogene palynomorph and radiolarian biostratigraphy of DSDP Leg 29, Sites 280 and 281, South Tasman Rise. *Inst. Geol. Nucl. Sci., Sci. Rep,* 96:1–46.

Duane, A.M., Pirrie, D., and Riding, J.B. (Eds.), 1992. Palynology of the James Ross Island area, Antarctic Peninsula. *Antarct. Sci.,* 4:257–362.

Edbrooke, S.W., Crouch, E.M., Morgans, H.E.G., and Sykes, R., 1998. Late Eocene–Oligocene Te Kuiti Group at Mount Roskill, Auckland, New Zealand. *N. Z. J. Geol. Geophys.,* 41:85–93.

Elliot, D.H., Askin, R.A., Kyte, F., and Zinsmeister, W.J., 1994. Iridium and dinocysts at the Cretaceous/Tertiary boundary on Seymour Island, Antarctica. *Geology,* 22:675–678.

Firth, J.V., 1996. Upper middle Eocene to Oligocene dinoflagellate biostratigraphy and assemblage variations in Hole 913B, Greenland Sea. *In* Thiede, J., Myhre, A.M., Firth, J.V., Johnson, G.L., and Ruddiman, W.F. (Eds.), *Proc. ODP, Sci. Results,* 151: College Station, TX (Ocean Drilling Program), 203–242.

Guerstein, G.R., Chiesa, J.O., Guler, M.V., and Camacho, H.H., 2002. Bioestratigrafia basada en quistes de dinoflagelados de la Formacion Cabo Pena (Eoceno terminal-Oligoceno temprano), Tierra del Fuego. *Argent. Rev. Esp. Micropal.,* 34:105–116.

Hannah, M.J., 1997. Climate controlled dinoflagellate distribution in late Eocene–earliest Oligocene strata from CIROS-01 drillhole, McMurdo Sound, Antarctica. *Terra Antart.,* 4:73–78.

Hannah, M.J., Cita, M.B., Coccioni, R., and Monechi, S., 1997. The Eocene/Oligocene boundary at 70º South, McMurdo Sound, Antartica. *Terra Antart.,* 4:79–87.

Hannah, M.J., and Raine, J.I. (Eds.), 1997. Southern Ocean Late Cretaceous/early Cenozoic biostratrigraphic datums: a report of the Southern Ocean paleontology workshop. *Sci. Rep.–Inst. Geol. Nucl. Sci.,* 4:1–33.

Hannah, M.J., Wilson, G.J., and Wrenn, J.H., 2000. Oligocene and Miocene marine palynomorphs from CRP-2/2A, Victorialand Basin, Antarctica. *Terra Antart.,* 7:503–511.

Hannah, M.J., Wrenn, J.H., and Wilson, G.J., 1998. Early Miocene and Quaternary marine palynomorphs from Cape Roberts project CRP-1, McMurdo Sound, Antarctica. *Terra Antart.,* 5:527–538.

Harland, R., FitzPatrick, M.E.J., and Pudsey, C.J., 1999. Latest Quaternary dinoflagellate cyst climatostratigraphy for three cores from the Falkland Trough, Scotia and Weddell Seas, Southern Ocean. *Rev. Palaeobot. Palynol.,* 107:265–281.

Harland, R., and Pudsey, C.J., 1999. Dinoflagellate cysts from sediment traps deployed in the Bellinghausen, Weddell and Scotian Seas, Antarctica. *Mar. Micropaleontol.,* 37:77–99.

———, 2002. Protoperidiniacean dinoflagellate cyst taxa from the upper Miocene of ODP Leg 178, Antarctic Peninsula. *Rev. Palaeobot. Palynol.,* 120:263–284.

Harland, R., Pudsey, C.J., Howe, J.A., and FitzPatrick, M.E.J., 1998. Recent dinoflagellate cysts in a transect from the Falkland Trough to the Weddell Sea, Antarctica. *Palaeontology,* 41:1093–1131.

Haskell, T.R., and Wilson, G.L., 1975. Palynology of Sites 280–284, DSDP Leg 29, off southeastern Australia and western New Zealand. *In* Kennett, J.P., Houtz, R.E., et al., *Init. Repts. DSDP,* 29: Washington (U.S. Govt. Printing Office), 731–741.

Levy, R.H., and Harwood, D.M., 2000. Tertiary marine palynomorphs from the McMurdo Sound erratics, Antarctica. *Antarct. Res. Ser.,* 76:183–242.

Mao, S., and Mohr, B.A.R., 1995. Middle Eocene dinocysts from Bruce Bank (Scotia Sea, Antarctica) and their palaeoenvironmental and palaeogeographic implications. *Rev. Palaeobot. Palynol.,* 86:235–263.

McMinn, A., Howard, W.R., and Roberts, D., 2001. Late Pliocene dinoflagellate cyst and diatom analysis from a high resolution sequence in DSDP Site 594, Chatham Rise, southwest Pacific. *Mar. Micropaleontol.,* 43:207–221.

Mohr, B.A.R., 1990. Eocene and Oligocene sporomorphs and dinoflagellate cysts from Leg 113 drill sites, Weddell Sea, Antarctica. *In* Barker, P.F., Kennett, J.P., et al., *Proc. ODP, Sci. Results,* 113: College Station, TX (Ocean Drilling Program), 595–612.

Pirrie, D., Duane, A.M., and Riding, J.B., 1992. Jurassic–Tertiary stratigraphy and palynology of the James Ross Basin: review and introduction. *Antarct. Sci.,* 4:259–266.

Powell, A.J., Brinkhuis, H., and Bujak, J.P., 1995. Upper Paleocene–lower Eocene dinoflagellate cyst sequence biostratigraphy of SE England. *In* Knox, R.W.O'B, Corfield, R., and Dunay, R.E. (Eds.), *Correlation of the Early Paleogene in Northwest Europe.* Spec. Publ.—Geol. Soc. London, 101:145–183.

Rochon, A., de Vernal, A., Turon, J.L., Mathiessen, J., and Head, M.J., 1999. Distribution of recent dinoflagellate cysts in surface sediments from the North Atlantic Ocean and adjacent seas in relation to sea-surface parameters. *Am. Assoc. Strat. Palynol. Found. Cont. Ser.,* 35.

Shafik, S., and Idnurm, M., 1997. Calcareous microplankton and polarity reversal stratigraphies of the upper Eocene Browns Creek clay in the Otway Basin, southeast Australia: matching the evidence. *Aust. J. Earth Sci.,* 44:77–86.

Shipboard Scientific Party, 2001a. Leg 189 summary. *In* Exon, N.F., Kennett, J.P., Malone, M.J., et al., *Proc. ODP, Init. Repts.,* 189, 1–98 [CD-ROM]. Available from: Ocean Drilling Program, Texas A&M University, College Station TX 77845-9547, USA.

————, 2001b. Site 1170. *In* Exon, N.F., Kennett, J.P., Malone, M.J., et al., *Proc. ODP, Init. Repts.,* 189, 1–167 [CD-ROM]. Available from: Ocean Drilling Program, Texas A&M University, College Station TX 77845-9547, USA.

————, 2001c. Site 1172. *In* Exon, N.F., Kennett, J.P., Malone, M.J., et al., *Proc. ODP, Init. Repts.,* 189, 1–149 [CD-ROM]. Available from: Ocean Drilling Program, Texas A&M University, College Station TX 77845-9547, USA.

Smith, S.W., 1992. Microplankton from the Cape Lamb member, López de Bertodano Formation (Upper Cretaceous), Cape Lamb, Vega Island. *Antarct. Sci.,* 4:337–353.

Stover, L.E., 1975. Observations on some Australian Eocene dinoflagellates. *Geoscience and Man. Proc. 6th Annu. Mtg. Am. Assoc. Stratigr. Palynol.,* 11:35–45.

Stover, L.E., Brinkhuis, H., Damassa, S.P., de Verteuil, L., Helby, R.J., Monteil, E., Partridge, A.D., Powell, A.J., Riding, J. B., Smelror, M., and Williams, G.L., 1996. Mesozoic–Tertiary dinoflagellates, acritarchs and prasinophytes. *In* Jansonius, J., and McGregor, D.C. (Eds.), *Principles and Applications* (Vol. 2): College Station, TX (Am. Assoc. Stratigraphic Palynol. Found.), 641–750.

Strong, C.P., Hollis, C.J., and Wilson, G.J., 1995. Foraminiferal, radiolarian, and dinoflagellate biostratigraphy of Late Cretaceous to middle Eocene pelagic sediments (Muzzle Group), Mead Stream, Marlborough, New Zealand. *N. Z. J. Geol. Geophys.,* 38:171–209.

Truswell, E.M., 1997. Palynomorph assemblages from marine Eocene sediments on the west Tasmanian continental margin and the South Tasman Rise. *Aust. J. Earth Sci.,* 44:633–654.

Williams, G.L., Lentin, J.K., and Fensome, R.A., 1998. *The Lentin and Williams Index of Fossil Dinoflagellate Cysts* (1998 ed.). Am. Assoc. Stratigr. Palynol., Contrib. Ser., 34.

Willumsen, P.S., 2000. Late Cretaceous to early Paleocene palynological changes in midlatitude Southern Hemisphere, New Zealand. *GFF,* 122:180–181.

Wilpshaar, M., Santarelli, A., Brinkhuis, H., and Visscher, H., 1996. Dinoflagellate cysts and mid-Oligocene chronostratigraphy in the central Mediterranean region. *J. Geol. Soc. London,* 153:553–561

Wilson, G.J., 1978. The dinoflagellate species *Isabelia druggii* (Stover) and *Isabelia seelandica* (Lange): their association in the Teurian of Woodside Creek, Marlborough, New Zealand. *N. Z. J. Geol. Geophys.,* 21:75–80.

————, 1984. Some new dinoflagellate species from the New Zealand Haumurian and Piropauan Stages (Santonian–Maestrichtian, Late Cretaceous). *N. Z. J. Bot.,* 22:549–556.

————, 1985. Dinoflagellate biostratigraphy of the Eocene Hampden Section, North Otago, New Zealand. *N. Z. Geol. Surv. Rec.,* 8:93–101.

————, 1988. Paleocene and Eocene dinoflagellate cysts from Waipawa, Hawkes Bay, New Zealand. *N. Z. Geol. Surv. Bull.,* 57:1–96.

Wrenn, J.H., and Beckmann, S.W., 1982. Maceral, total organic carbon, and palynological analyses of Ross Ice Shelf Project site J9 cores. *Science,* 216:187–189.

Wrenn, J.H., Hannah, M.J., and Raine, J.I., 1998. Diversity and palaeoenvironmental significance of late Cainozoic marine palynomorphs from the CRP-1 core, Ross Sea, Antarctica. *Terra Antart.,* 5:553–570.

Wrenn, J.H., and Hart, G.F., 1988. Paleogene dinoflagellate cyst biostratigraphy of Seymour Island, Antarctica. *Mem.—Geol. Soc. Am.,* 169:321–447.

APPENDIX

Species List and Taxonomic Remarks

Achilleodinium spp.

Achomosphaera alcicornu

Adnatosphaeridium multispinosum

Aiora fenestrata

Aireiana verrucosa

Algidasphaeridium minutum var. *cezare*

Algidasphaeridium minutum var. *minutum*

Alisocysta circumtabulata

Alisocysta margarita

Alisocysta reticulata group
    Remarks: In this group, morphologically closely related forms assignable to *Alisocysta reticulata*, *Cassidium* spp., and *Eisenackia crassitabulata* are combined (cf. Crouch, 2001).

Alterbidinium acutulum

Alterbidinium distinctum

Alterbidinium spp. (pars)
    Remarks: This group is combined with the morphologically closely related *Diconodinium* spp. in the case of Hole 1172D analyses. The latter differ from *Alterbidinium* spp. in being essentially acavate.

Apectodinium homomorphum

Arachnodinium antarcticum

Areoligera? semicirculata

Ataxiodinium choane

Batiacasphaera spp.
    Remarks: This group constitutes several new species, to be formally described elsewhere.

Bitectatodinium tepekiense

Brigantedinium? sp.
    Remarks: This species is throughout comparable to species of *Brigantedinium*, but differs by having a distinct periphragm, in ideally preserved cases displaying a long, slender apical horn, besides two long and slender antapical horns. The length of the horns may be as much as four times the diameter of the central body. This outer wall is delicate and thin, and is often either removed though oxidation or mechanical disturbance or may be present as a wrinkled, poorly defined thin outer membrane. Since *Brigantedinium* species are considered acavate, the species is questionably attributed here to the genus. The species is most probably conspecific with forms depicted by Mohr (1990) as "*Brigantedinium* sp." from sediments with a similar age off Seymour Island (DSDP Site 696). The species will be formally described elsewhere.

Brigantedinium spp.

Cerebrocysta spp.
    Remarks: This group constitutes several new species, to be formally described elsewhere.

Cerodinium sp. A

Remarks: This taxon has a characteristic elongate shape with outward-pointing, short antapical horns and is here separated from other forms, grouped as *Cerodinium* spp. It is apparently restricted to the Maastrichtian interval, and is possibly conspecific with *Broomea*? sp. of Askin (1988a) and/or *Cerodinium* sp. A of Smith (1992). The species will be formally described elsewhere.

Cerodinium spp. (pars.)

Charlesdowniea coleothrypta

Charlesdowniea edwardsii group
    Remarks: Forms whose morphology ranges between *C. edwardsii* and *Charlesdowniea columna* are combined in this group.

Circulodinium compactum

Cleistosphaeridium spp.

Cordosphaeridium fibrospinosum group

Cordosphaeridium minimum

Corrudinium spp.
    Remarks: This group constitutes several new species, to be formally described elsewhere.

Cribroperidinium sp. A.
    Remarks: This taxon is morphologically comparable to *Impagidinium waipawaensis* of Wilson (1988), but differs by lacking perforations in the parasutural ridges. The dextral torsion warrants attribution to *Cribroperidinium*. The species will be formally described elsewhere.

Cribroperidinium spp. (pars.)

Dapsilidinium spp.

Deflandrea antarctica group
    Remarks: Forms morphologically ranging between *D. antarctica* and *Deflandrea cygniformis* are combined in this group (essentially all forms with a distinct bell-shaped hypotract and short antapical horns).

Deflandrea convexa group
    Remarks: Forms of *Deflandrea* characterized by a condensed periphragm are combined in this group.

Deflandrea phosphoritica group
    Remarks: Forms of *Deflandrea* characterized by having a periphragm corresponding to the general periphragmal outline of *D. phosphoritica* are combined in this group, regardless of ornamentation of the periphragm and/or endophragm (e.g., including *D. granulosa, D. granulata, D. robusta, D. spinosa, D. heterophlycta,* and *D. webbii*)

Deflandrea sp. A
    Remarks: This rather large species of *Deflandrea* may be characterized by a distinctly triangular endophragm and by having a relatively long apical and short antapical horns. It is possibly partly conspecific with *Deflandrea prydzensis* (manuscript name) of Truswell, 1997. The species will be formally described elsewhere.

Diconodinium spp.
    Remarks: This group constitutes several new species, to be formally described elsewhere.

Dinogymnium spp.

Dinopterygium sp. A
    Remarks: This species of *Dinopterygium* closely resembles *Dinoptergium cladoides* pending the concept used of the latter. Further study will further elucidate morphological relationships. In any event, representatives of *Dinoptery-*

gium sensu stricto have never been reported from deposits as young as latest Maastrichtian in age. The species will be formally described elsewhere.

Dinopterygium spp. (pars.)
  Remarks: Specimens assigned to *Dinopterygium* spp. (pars.) are relatively small representatives of the genus. Many of these are assignable to "*Dinopterygium cladoides sensu* Morgenroth."

Diphyes colligerum

Diphyes ficusoides

Distatodinium spp.

Dracodinium waipawaense

Echinidinium spp.

Elytrocysta spp.

Enneadocysta partridgei

Enneadocysta pectiniformis

Enneadocysta sp. A
  Remarks: This species of *Enneadocysta* closely resembles *Areosphaeridium diktyoplokum* but differs by having two antapical processes, distally united by a single perforated platform, and by being dorso-ventrally compressed. The latter features are more typical for *Enneadocysta*, although clearly the form (and other species of *Enneadocysta*) is/are gonyaulacoid sexiform rather than partiform as suggested by Stover and Williams (1995). The species will be formally described elsewhere.

Eocladopyxis spp.
  Remarks: This group constitutes several new species, to be formally described elsewhere.

Exochosphaeridium bifidum

Fibrocysta axialis

Florentinia mantellii

Gelatia inflata

Glaphyrocysta spp.
  Remarks: This group constitutes several new species, to be formally described elsewhere.

Hafniasphaera septata

Hemiplacophora semilunifera

Heteraulacacysta spp.

Histiocysta spp.

Homotryblium spp.

Hystrichokolpoma bullatum

Hystrichokolpoma eisenackii

Hystrichokolpoma rigaudiae

Hystrichokolpoma spinosum

Hystrichokolpoma truncatum

Hystrichokolpoma sp. cf. *Homotryblium oceanicum* Wilpshaar et al., 1996

Hystrichosphaeridium truswelliae

Hystrichosphaeridium tubiferum

Hystrichosphaeropsis spp.

Hystrichostrogylon spp.

Impagidinium spp.
   Remarks: This group constitutes several new species, to be formally described elsewhere.

Isabelidinium spp.

Kallosphaeridium spp.

Lejeunecysta spp.

Lingulodinium machaerophorum

Manumiella spp.

Melitasphaeridium pseudorecurvatum

Membranophoridium perforatum

Nematosphaeropsis spp.

Octodinium askiniae

Odontochitina operculata

Oligosphaeridium spp.

Operculodinium? sp. A
   Remarks: This taxon is provisionally assigned to *Operculodinium*. This in view of it having only very short spines and a quasi-reticulate thick periphragm atypical of the genus. The species will be formally described elsewhere.

Operculodinium spp. (pars.)

Palaeocystodinium spp.

Palaeoperidinium pyrophorum

Paucisphaeridium spp.
   Remarks: This group constitutes several new species, to be formally described elsewhere.

Pentapharsodinium dalei cysts

Pentadinium laticinctum

Phelodinium kozlowskii

Phthanoperdinium echinatum group

Phthanoperidinium spp.
   Remarks: This group constitutes several new species, to be formally described elsewhere.

Polykrikos schwartzii

Polysphaeridium spp.

Pyxidinopsis spp.
   Remarks: This group constitutes several new species, to be formally described elsewhere.

Reticulatosphaera actinocoronata

Rottnestia borussica

Samlandia chlamydophora

Samlandia delicata group

Schematophora obscura

Schematophora speciosa

Senegalinium bicavatum

Senegalinium dilwynense

Selenopemphix nephroides

Selenopemphix quanta

Senoniasphaera inornata

Spinidinium luciae

Spinidinium macmurdoense

Spinidinium spp. (pars.)
   Remarks: This group constitutes several new species, to be formally described elsewhere.

Spiniferella cornuta

Spiniferites pseudofurcatus

Spiniferites mirabilis

Spiniferites cf. *mirabilis*
   Remarks: This taxon resembles *S. mirabilis* but differs by having a much larger size range (up to 120 μm) and by less well defined and developed processes.

Spiniferites sp. A
   Remarks: This species of *Spiniferites* is characterized by it having septate processes, distally expanding into a broad trifurcation a la *Spiniferites pseudofurcatus*. It is however much smaller than typical *S. pseudofurcatus*. The species will be formally described elsewhere.

Spiniferites sp. B
   Remarks: This species of *Spiniferites* is characterized by it having (1) intergonal bifurcate processes and (2) sutural ridges that are higher at gonal junctions, giving the cyst broad arch-shaped sides. The species will be formally described elsewhere.

Spiniferites spp. (pars.)

Stelladinium stellatum

Stoveracysta kakanuiensis

Stoveracysta ornata

Tanyosphaeridium spp.

Tectatodinium spp.

Thalassiphora delicata

Thalassiphora pelagica

Trithyrodinium evittii

Turbiosphaera filosa

Vozzhennikovia spp.
   Remarks: This group constitutes several new species, to be formally described elsewhere.

Wetzeliella articulata

Wetzeliella spp. (pars.)

Wilsonidium compactum

Wilsonidium echinosuturatum

Wilsonidium ornatum

Figure F1. ODP Leg 189 drilling locations (Sites 1168–1172).
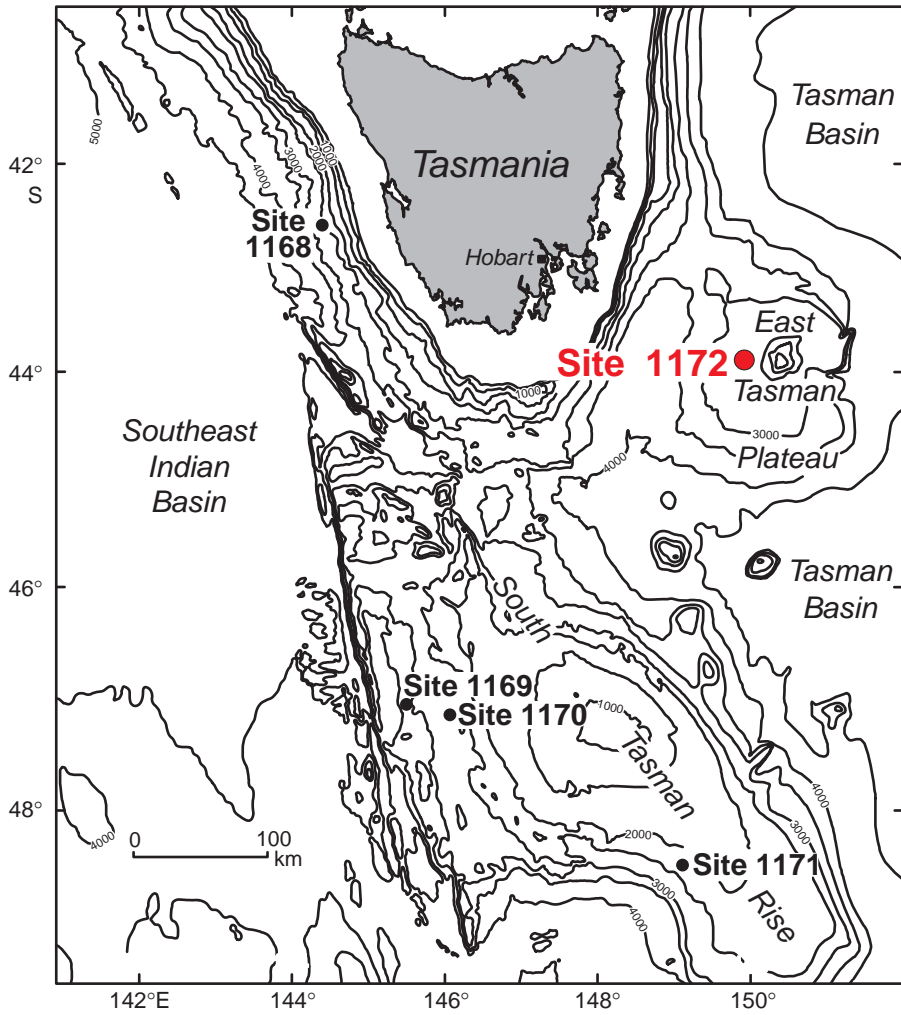
Figure F2. Percentage of terrestrial palynomorphs and percentage of offshore (oceanic) dinocysts (marked "o" in Tables **T2,** p. 26, and **T3,** p. 27) in palynological assemblages of Holes 1172A and 1172D. TD = total depth.
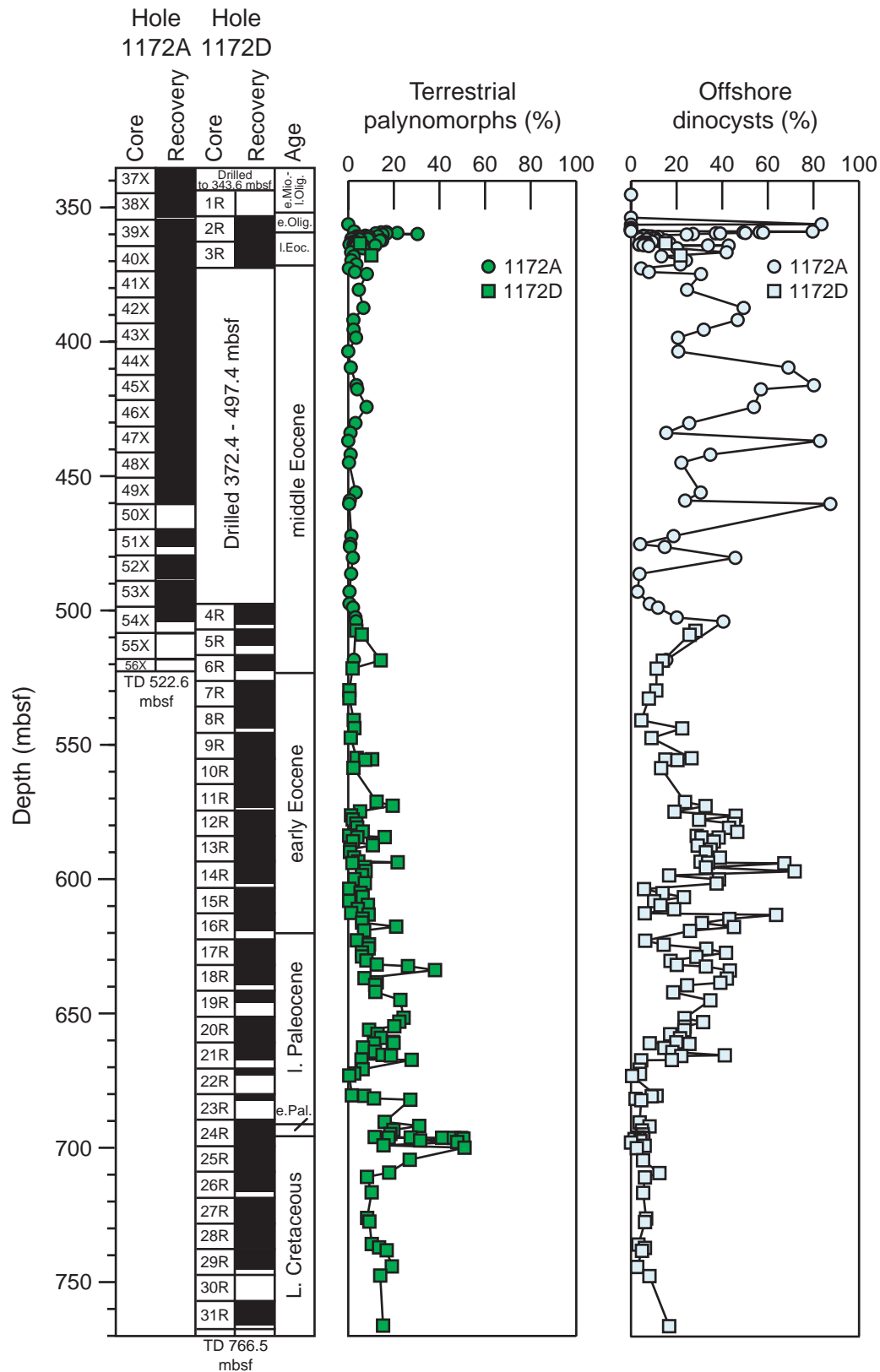
Table T1. A selection of palynological results from samples, Hole 1172A, part 1: Quaternary. (Continued on next page.)

Core, section, interval (cm)	Depth (mbsf)	Age (Ma)	N (reworked)	N (acritarchs)	N (copepod eggs)	N (foraminifer linings) (spiral)	N (fungal spores)	N (spores)	N (bi-/trisaccates)	N (other pollen)	N (Cymatiospaera)	N (total palynomorphs excl. DC)	N (indet. dinocysts) (1st count)	N (det. dinocysts) (1st count)	Total palynomorphs (1st count)	Total dinocysts (2nd count)	Ataxiodinium choanum	Algidasphaeridium minutum var. minutum	Algidasphaeridium minimum var. cezare	Brigantedinium spp.	Bitectatodinium tepekiense	Dalella chathamiense	Echinidinium spp.	Impagidinium aculeatum
189-1172A-																								
1H-1, 85–87	0.86	~0.006	0	0	0	41	0	23	4	8	0	76	5	119	200	200	1	0	0	49	0	0	0	2
1H-2, 85–87	2.35	~0.183	0	2	2	11	3	31	5	5	0	59	0	141	200	200	0	0	0	3	1	0	0	2
1H-3, 85–87	3.85	~0.336	1	0	0	3	0	60	4	3	1	71	1	128	200	200	0	0	0	0	0	1	0	67.5
1H-4, 85–87	5.35	~0.377	0	0	1	45	0	33	7	6	1	93	0	107	200	200	2	1	0	15	0	0	0	27
2H-1, 85–87	7.15	~0.441	0	0	5	66	2	30	5	1	0	109	0	91	200	200	1	0	0	13	0	0	0	11
2H-2, 85–87	8.65	~0.513	0	0	1	42	2	28	7	2	1	82	0	118	200	200	0	0	0	5	0	0	0	9
2H-3, 85–87	10.15	~0.549	0	0	4	60	3	37	10	6	0	120	6	74	200	199.5	0	12	10	35	0	0	1	9
2H-4, 85–87	11.65	~0.64	0	0	0	51	0	35	3	7.5	1	97.5	0	102.5	200	200	1	3	0	72	0	0	0	1
2H-5, 85–87	13.15	~0.85	0	0	1	0	2	45	5	7	0	60	1	139	200	200	0	0	0	0	0	0	0	45
2H-6, 85–87	14.65	~0.87	0	0	2	28	0	64	8	5	0	107	0	93	200	199.5	0	1	1	7	0	0	1	10
3H-1, 59–61	16.39	?1.50	0	0	0	24	0	26.5	1	3	0	56.5	0	143.5	200	200.25	1	0	0	8	1	1	1	8
3H-3, 85–87	19.65	~1.95	2	1	2.5	29	0	28.5	2	7	0	70.5	2	127.5	200	199.5	1	1	0	19	0	0	0	33
3H-4, 85–87	21.15	?2.0	0	0	1	13	0	26	6	6	3	55	2	145	200	200	2	5	12	1	0	0	0	11
3H-5, 85–87	22.65	?2.1	1.5	1	3	35	2	36	8	5	1	91	4	105	200	200.5	2	16	4	0	0	0	2	17.5
3H-6, 85–87	24.15	?2.2	0	0	0	14	7	9	3	0	7	40	2.75	157.25	200	200.25	2	0	0	0	0	0	1	15

Notes: Ages are derived from Stickley et al. (this volume). *N* = number. DC = dinocysts.

Table T1 (continued).

Core, section, interval (cm)	Impagidinium japonicum	Impagidinium pallidum	Impagidinium paradoxum	Impagidinium patulum	Impagidinium sphaericum	Impagidinium strialatum	Impagidinium spp. (pars.)	Lingulodinium machaerophorum	Lejeunecysta spp.	Nematosphaeropsis spp.	Operculodinium spp.	Pentapharsodinium dalei cysts	Pyxidinopsis spp.	Polykrikos schwartzii	Selenopemphix nephroides	Selenopemphix quanta	Spiniferites mirabilis	Spiniferites cf. mirabilis	Spiniferites spp. (pars.)	Indet. dinocysts
189-1172A-																				
1H-1, 85–87	0	0	2	12	0	0	20	0	4	62	1	0	0	1	0	0	10	4	23	9
1H-2, 85–87	1	1	6	9	5	0	9	0	1	104	5	3	0	0	0	0	5	3	42	0
1H-3, 85–87	0	0	3	6	3	0	5.5	0	0	27	7	1	5.5	0	0	2	38	12	20.5	1
1H-4, 85–87	3	0	6.5	11	3	0	9	2	3	57	0	0	7	0	4	29	0	9	11.5	0
2H-1, 85–87	1	0	10	10	2	1	9	0	2	45	10	0	2	0	4	0	30	20	26	3
2H-2, 85–87	0	0	8	5.5	1	0	6	0	1	26	10	1	5	0	3	0	23	44.5	52	0
2H-3, 85–87	2	1	9.5	2	1	1	12	0	5.25	24	24.75	6	9	0	0	1	5	3	20	6
2H-4, 85–87	0	0	2	1	0	0	2	0	13	12	7	2	12	0	6	7	18	10	29	2
2H-5, 85–87	0	0	11	13	7	1	5	0	0	62	7	1	22	0	0	3	13	0	9	1
2H-6, 85–87	3	0	8	9	2	0	3.5	0	0	58	3	0	31	0	1	0	14	4	43	0
3H-1, 59–61	5	0	23.5	4.5	4	0	2	0	0	35	9	1.5	8	0	1	3.5	24	24	34.25	1
3H-3, 85–87	7	0	30	7.5	0	0	0	4	0	31	6.5	2	1	0	0	0	15	0	40.5	1
3H-4, 85–87	0	0	11	0	3	0	0	0	2	78	15	10	0	0	0	0	9	0	39	2
3H-5, 85–87	0	0	20	0	2	0	3	1	2	6	8	23.5	0	0	2.5	1	33	0	52.75	4.25
3H-6, 85–87	0	1	3	0	0	1	1	0.25	0	10	6.5	9	0	0	0.5	0	50	0	97.25	2.75

Table T2. A selection of palynological results from samples, Hole 1172A, part 2: Eocene–Oligocene. (This table is available in an **oversized format.**)

Table T3. A selection of palynological results from samples, Hole 1172D, Maastrichtian–Eocene. (This table is available in an **oversized format.**)

Table T4. Selected potentially age-indicative dinocyst events, Holes 1172A and 1172D. (**See table note.** Continued on next page.)

Dinocyst datum	Core, section, interval (cm)		Depth (mbsf)				Magnetochron	Magneto age (Ma)
	Top	Bottom	Top	Bottom	Mean	Error		
189-1172A-								
LO *Enneadocysta partridgei* (?)	38X-CC, 24–29	39X-2, 3–5	353.76	356.13	354.945	1.185	C11n	31
FO *Hystrichokolpoma* sp. cf. *H. oceanicum*	38X-CC, 24–29	39X-2, 3–5	353.76	356.13	354.945	1.185	C11n	31
LO *Spinidinium macmurdoense* (?)	39X-3, 122–124	39X-3, 145–147	358.82	359.05	358.935	0.115	C13r	33.5
LO *Octodinium askiniae* (?)	39X-3, 122–124	39X-3, 145–147	358.82	359.05	358.935	0.115	C13r	33.5
FO *Spiniferites mirabilis*	39X-3, 122–124	39X-3, 145–147	358.82	359.05	358.935	0.115	C13r	33.5
LO *Alterbidinium distinctum* (?)	39X-3, 122–124	39X-3, 145–147	358.82	359.05	358.935	0.115	C13r	33.5
LO *Enneadocysta* sp. A (?)	39X-3, 122–124	39X-3, 145–147	358.82	359.05	358.935	0.115	C13r	33.5
LO *Stoveracysta kakanuiensis* (?)	39X-3, 122–124	39X-3, 145–147	358.82	359.05	358.935	0.115	C13r	33.5
LO *Turbiosphaera filosa* (?)	39X-3, 122–124	39X-3, 145–147	358.82	359.05	358.935	0.115	C13r	33.5
LO *Vozzhennikovia* spp.	39X-3, 122–124	39X-3, 145–147	358.82	359.05	358.935	0.115	C13r	33.5
FO *Reticulatosphaera actinocoronata*	39X-4, 10–12	39X-4, 25–27	359.2	359.35	359.275	0.075	C13r	33.5
FO *Stoveracysta kakanuiensis*	39X-4, 40–42	39X-4, 45–47	359.51	359.56	359.535	0.025	C13r	33.5
FO *Deflandrea* sp. A	39X-4, 85–87	39X-4, 130–132	359.95	360.4	360.175	0.225	C16n1n	35.4
LO *Schematophora speciosa*	39X-4, 130–132	39X-4, 147–149	360.4	360.57	360.485	0.085	C16n1n	35.4
LO *Spinidinium luciae*	39X-5, 10–12	39X-5, 17–19	360.7	360.77	360.735	0.035	C16n1n	35.4
LO *Aireiana verrucosa*	39X-5, 17–19	39X-5, 22–24	360.77	360.82	360.795	0.025	C16n1n	35.4
LO *Hemiplacophora semilunifera*	39X-5, 17–19	39X-5, 22–24	360.77	360.82	360.795	0.025	C16n1n	35.4
FO *Gelatia inflata*	39X-5, 22–24	39X-5, 55–57	360.82	361.15	360.985	0.165	C16n1n	35.4
FO *Aireiana verrucosa*	39X-5, 55–57	39X-5, 85–87	361.15	361.45	361.3	0.15	C16n2n	35.7
FO *Schematophora speciosa*	39X-5, 85–87	39X-5, 100–102	361.45	361.6	361.525	0.075	C16n2n	35.7
FO *Achomosphaera alcicornu*	39X-6, 5–7	39X-6, 10–12	362.15	362.2	362.175	0.025	C16n2n	35.7
LOA *Enneadocysta* spp.	39X-7, 31–33	39X-7, 40–42	363.92	364.01	363.965	0.045	C16n2n	35.7
FCO *Alterbidinium distinctum*	39X-CC, 27–33	40X-1, 85–87	364.34	365.05	364.695	0.355	C16n2n	35.7
LO *Pyxidinopsis waipawaensis* group	39X-CC, 27–33	40X-1, 85–87	364.34	365.05	364.695	0.355	C16n2n	35.7
FOA *Spinidinium macmurdoensis*	40X-2, 85–87	40X-3, 85–87	366.56	368.06	367.31	0.75	C16r2r	36.4
FO *Stoveracysta ornata*	40X-3, 85–87	40X-4, 85–87	368.05	369.55	368.8	0.75	C16r2r	36.4
LO *Wilsonidium ornatum*	40X-CC, 26–31	41X-1, 85–87	374	374.65	374.325	0.325	C17n	37
LO *Arachnodinium antarcticum*	41X-5, 86–88	42X-3, 85–87	380.51	387.25	383.88	3.37	C18n1n	38.8
LO *Hystrichosphaeridium truswelliae*	41X-5, 86–88	42X-3, 85–87	380.51	387.25	383.88	3.37	C18n1n	38.8
LO *Hystrichokolpoma spinosum*	42X-6, 85–87	43X-2, 85–87	391.75	395.35	393.55	1.8	C18n1n	38.8
FO *Hemiplacophora semilunifera*	46X-6, 85–87	47X-2, 85–87	430.15	433.75	431.95	1.8	C19n	41.3
LO *Spiniferites* sp. B	47X-2, 85–87	47X-4, 85–87	433.75	436.75	435.25	1.5	C19r	42
LO *Wilsonidium echinosuturatum*	47X-2, 85–87	47X-4, 85–87	433.75	436.75	435.25	1.5	C19r	42
FO *Batiacasphaera compta*	50X-CC, 0–8	51X-2, 85–87	460.2	472.15	466.175	5.975	C20r	44.5
LCO *Deflandrea convexa* group	53X-CC, 34–39	54X-3, 85–87	498.8	502.45	500.625	1.825	C20r	44.5
189-1172D-								
FO *Wilsonidium echinosuturatum*	5R-1, 40–42	5R-2, 38–40	507.4	508.88	508.14	0.74	C21n	46.6
FCO *Enneadocysta* sp. A	5R-2, 38–40	6R-2, 38–40	508.88	518.48	513.68	4.8	C21n	46.6
FCO *Enneadocysta partridgei*	6R-4, 38–40	7R-3, 40–42	521.48	529.6	525.54	4.06	C21r	48.5
LO *Membranophoridium perforatum*	6R-4, 38–40	7R-3, 40–42	521.48	529.6	525.54	4.06	C21r	48.5
LO *Charlesdowniea edwardsii/columna*	8R-6, 40–42	9R-2, 40–42	534.7	547.3	541	6.3	C22r	50
LO *Cribroperidinium* sp. A	9R-2, 40–42	9R-7, 40–42	547.3	554.8	551.05	3.75	C22r	50
FOA *Vozzhennikovia* spp.	9R-7, 40–42	9R-CC, 15–22	554.8	555.295	555.0475	0.2475	C22r	50
LO *Batiacasphaera cassicula*	10R-1, 40–42	10R-3, 40–42	555.5	558.5	557	1.5	C23n1n	50.8
FO *Arachnodinium antarcticum*	10R-3, 40–42	11R-5, 40–42	558.5	571.1	564.8	6.3	C23n2n	51.4
LO *Melitasphaeridium pseudorecurvatum*	10R-3, 40–42	11R-5, 40–42	558.5	571.1	564.8	6.3	C23n2n	51.4
FOA *Phthanoperdinium echinatum* group	10R-3, 40–42	11R-5, 40–42	558.5	571.1	564.8	6.3	C23n2n	51.4
FO *Charlesdowniea edwardsii/columna*	11R-5, 40–42	11R-6, 40–42	571.1	572.6	571.85	0.75	C23r	52
LO *Thalassiphora delicata*	11R-5, 40–42	11R-6, 40–42	571.1	572.6	571.85	0.75	C23r	52
LO *Dracodinium waipawaense*	12R-4, 40–42	12R-5, 40–42	579.21	580.71	579.96	0.75	C23r	52
LO *Impagidinium cassiculum*	12R-4, 40–42	12R-5, 40–42	579.21	580.71	579.96	0.75	C23r	52
FO *Hystrichokolpoma rigaudiae*	12R-CC, 23–28	13R-1, 40–42	584.27	584.31	584.29	0.02	C24n1n	52.4
FO *Hystrichokolpoma spinosum*	12R-CC, 23–28	13R-1, 40–42	584.27	584.31	584.29	0.02	C24n1n	52.4
FO *Hystrichokolpoma truncatum*	12R-CC, 23–28	13R-1, 40–42	584.27	584.31	584.29	0.02	C24n1n	52.4
LO *Cerodinium medcalfii*	13R-1, 40–42	13R-2, 40–42	584.31	585.81	585.06	0.75	C24n1n	52.4
FO *Membranophoridium perforatum*	13R-1, 40–42	13R-2, 40–42	584.31	585.81	585.06	0.75	C24n1n	52.4
LOA *Palaeocystodinium* spp.	13R-2, 40–42	13R-3, 40–42	585.81	587.31	586.56	0.75	C24r1r	52.6
FO *Cribroperidinium* sp. A	13R-5, 40–42	13R-6, 40–42	589.81	591.81	590.81	1	C24n2n	52.757
FO *Dracodinium waipawaense*	13R-5, 40–42	13R-6, 40–42	589.81	591.81	590.81	1	C24n2n	52.757
FO *Batiacasphaera cassicula*	13R-6, 40–42	13R-7, 40–42	591.81	593.31	592.56	0.75	C24n3n	53.1
FO *Octodinium askinae*	15R-3, 40–42	15R-4, 40–42	606.51	608.01	607.26	0.75	C24r3r	53.5
FO *Melitasphaeridium pseudorecurvatum*	15R-3, 40–42	15R-4, 40–42	606.51	608.01	607.26	0.75	C24r3r	53.5
FO *Thalassiphora pelagica*	15R-3, 40–42	15R-4, 40–42	606.51	608.01	607.26	0.75	C24r3r	53.5
FO *Deflandrea convexa* group	15R-4, 40–42	15R-5, 40–42	608.01	609.51	608.76	0.75	C24r3r	53.5
LO *Aiora fenestrata*	15R-5, 40–42	15R-6, 40–42	609.51	611.01	610.26	0.75	C24r3r	53.5

Table T4 (continued).

	Core, section, interval (cm)		Depth (mbsf)					Magneto age (Ma)
Dinocyst datum	Top	Bottom	Top	Bottom	Mean	Error	Magnetochron	
LCO *Alisocysta margarita*	15R-7, 40–42	16R-1, 40–42	612.51	613.11	612.81	0.3	C24r3r	53.5
FCO *Deflandrea phosphoritica* group	16R-1, 40–42	16R-2, 40–42	613.11	614.61	613.86	0.75	C24r3r	54
FO *Pentadinium laticinctum*	16R-1, 40–42	16R-2, 40–42	613.11	614.61	613.86	0.75	C24r3r	54
LCO *Alisocysta reticulata* group	16R-3, 40–42	16R-4, 40–42	616.11	617.61	616.86	0.75	C24r3r	54.5
FO *Apectodinium homomorphum*	17R-1, 40–42	17R-2, 40–42	622.71	624.21	623.46	0.75	C25n	56
FCO *Deflandrea antarctica* group	17R-4, 40–42	17R-5, 40–42	627.21	628.71	627.96	0.75	C25n	56
LO *Tanyosphaeridium* spp.	17R-4, 40–42	17R-5, 40–42	627.21	628.71	627.96	0.75	C25n	56
LO *Cerodinium* spp.	17R-5, 40–42	17R-6, 40–42	628.71	630.21	629.46	0.75	C25n	56
FO *Spinidinium macmurdoensis*	18R-2, 40–42	18R-4, 40–42	633.78	636.8	635.29	1.51	C25r	57
LCO *Alisocysta circumtabulata*	19R-3, 40–42	20R-1, 40–42	644.9	651.51	648.205	3.305	C25r	57
LO *Oligosphaeridium* spp.	19R-3, 40–42	20R-1, 40–42	644.9	651.52	648.21	3.31	C25r	57
FO *Diphyes colligerum*	20R-4, 40–42	20R-5, 40–42	656	657.51	656.755	0.755	C25r	57
LOA *Glaphyrocysta/Areoligera* spp.	20R-7, 40–42	20R-CC, 7–12	660.51	660.875	660.6925	0.1825	C25r	57
LO *Senegalinium dilwynense*	21R-4, 40–42	21R-5, 40–42	665.6	667.1	666.35	0.75	C25r	57
FO *Impagidinium victorianum*	21R-5, 40–42	21R-CC, 5–11	667.1	667.2	667.15	0.05	C25r	57
FO *Pyxidinopsis waipawaensis* group	21R-5, 40–42	21R-CC, 5–11	667.1	667.2	667.15	0.05	C25r	57
FO *Spiniferites* sp. B	21R-5, 40–42	21R-CC, 5–11	667.1	667.2	667.15	0.05	C25r	57
FO *Hystrichosphaeridium truswelliae*	23R-1, 41–43	23R-CC, 28–33	680.42	682.06	681.24	0.82	C25r	57
FO *Impagidinium cassiculum*	23R-1, 41–43	23R-CC, 28–33	680.42	682.06	681.24	0.82	C25r	57
FO *Thalassiphora delicata*	23R-1, 41–43	23R-CC, 28–33	680.42	682.06	681.24	0.82	C25r	57.3
LO *Trithyrodinium evittii*	23R-2, 4–8	23R-CC, 28–33	681.56	682.06	681.81	0.25	C25r	57.3
LO *Alterbidinium acutulum*	23R-CC, 28–33	24R-5, 12–14	682.06	695.93	688.995	6.935	C25r	57.3
FO *Cerodinium medcalfii*	23R-CC, 28–33	24R-5, 12–14	682.06	695.93	688.995	6.935	C25r	57.3
FOA *Glaphyrocysta/Areoligera* spp.	23R-CC, 28–33	24R-5, 12–14	682.06	695.93	688.995	6.935	C25r	57.3
LO *Operculodinium*? sp. A	23R-CC, 28–33	24R-5, 12–14	682.06	695.93	688.995	6.935	C25r	57.3
LOA *Palaeoperidinium pyrophorum*	23R-CC, 28–33	24R-1, 60–64	682.06	690.3	686.18	4.12	?C28	63?
LO *Senoniasphaera inornata*	24R-1, 60–64	24R-2, 60–64	690.3	691.8	691.05	0.75	?C28	63?
LOA *Manumiella* spp.	24-5, 36–38	24R-5, 40–42	696.17	696.21	696.19	0.02	C29n	64.7
LO *Spiniferites* sp. A	24R-5, 36–38	24R-5, 40–42	696.17	696.21	696.19	0.02	C29n	64.7
FOA *Palaeoperidinium pyrophorum*	24R-5, 40–42	24R-5, 44–46	696.21	696.25	696.23	0.02	C29n	64.7
FO *Senoniasphaera inornata*	24R-5, 40–42	24R-5, 44–46	696.21	696.25	696.23	0.02	C29n	64.7
FO *Trithyrodinium evittii*	24R-5, 40–42	24R-5, 47–48	696.21	696.275	696.2425	0.0325	C29/30n	64.7–65.5
LO *Dinopterygium* sp. A	24R-5, 44–46	24R-5, 47–48	696.25	696.275	696.2625	0.0125	C29/30n	64.7–65.6
FO *Cerodinium speciosum/striatum*	24R-CC, 0–6	25R-CC, 14–20	699.02	709.17	704.095	5.075	C30n	66
LO *Odontochitina operculata*	27R-7, 40–42	28R-6, 40–42	727.4	735.77	731.585	4.185	C31n	68.5
FO *Alisocysta reticulata* group	28R-6, 40–42	28R-7, 40–42	735.77	737.01	736.39	0.62	C31n	68.5
FO *Alisocysta circumtabulata*	28R-6, 40–42	28R-7, 40–42	735.77	737.01	736.39	0.62	C31n	68.5
FO *Dinopterygium* sp. A	30R-CC, 15–22	31R-CC, 17–22	747.5	766.14	756.82	9.32	C31r	69
FOA *Manumiella* spp.	31R-CC, 17–22	bottom	766.14	770	768.07	1.93	C31r	69

Note: LO = last occurrence, FO = first occurrence, LCO = last common occurrence, FCO = first common occurrence, LOA = last occurrence of abundant, FOA = first occurrence of abundant.

Plate P1. Illustrations of taxa, sample, and slide number. Scale bar = ~20 µm unless stated otherwise. Scanning electron microscope (SEM) photographs have varying scale bars. **1.** *Adnatosphaeridium multispinosum* (Sample 189-1172D-15R-3, 40–42cm) (1). **2.** *Aiora fenestrata* (Sample 189-1172D-15R-3, 40–42cm) (1); scale bar = ~15 µm. **3, 4.** *Aireiana verrucosa* (Sample 189-1172A-39X-5, 55–57 cm) (1). **5–7.** *Alisocysta circumtabulata;* (5) Sample 189-1172A-46X-2, 85–87 cm (1). (6, 7) Sample 189-1172D-21R-4, 15–18 cm (1); scale bar = ~15 µm. **8, 9.** *Alisocysta margarita* (Sample 189-1172D-16R-2, 40–42 cm) (1); scale bar = ~15 µm. **10, 11.** *Alisocysta reticulata* group (Sample 189-1172D-20R-1, 40–42 cm) (1); scale bar = ~15 µm. **12.** *Alisocysta reticulata* group (*Cassidium fragile*) (Sample 189-1172D-20R-5, 40–43 cm) (1); scale bar = ~10 µm. (Continued on next 17 pages.)
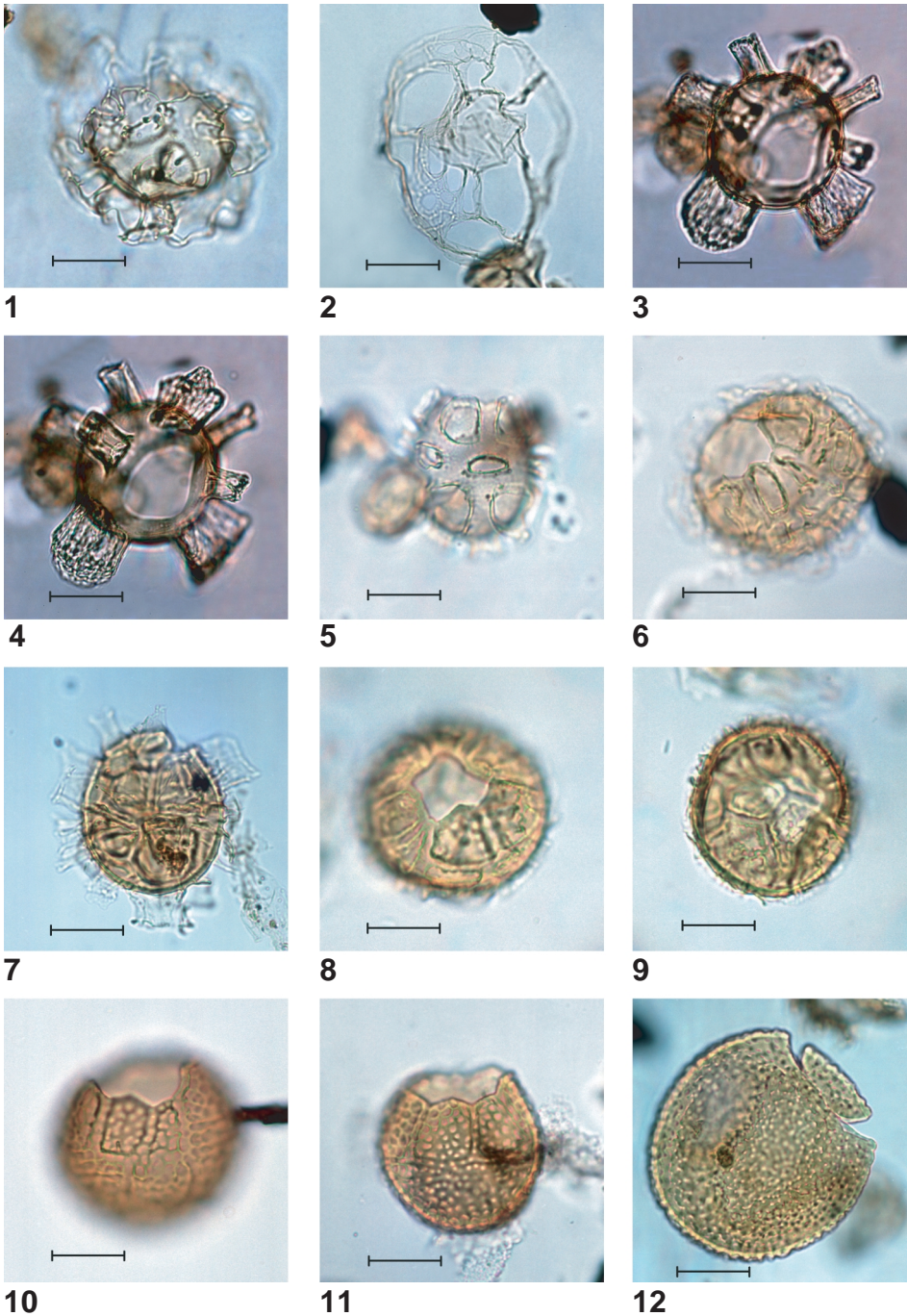
Plate P1 (continued). 13. *Alterbidinium acutulum* (Sample 189-1172D-24R-5, 130–133 cm) (1); scale bar = ~15 µm. **14.** *Alterbidinium distinctum* (Sample 189-1172A-39X-4, 85–87 cm) (2). **15–17.** *Arachnodinium antarcticum* (Sample 189-1172A-48-3, 85–87 cm) (1). **18, 19.** *Batiacasphaera cassicula* (Sample 189-1172D-10R-1, 40–42 cm) (1). **20–22.** *Brigantedinium*? sp. (Sample 189-1172A-39X-3, 128–130 cm) (2); scale bar = ~15 µm. Note periphragm delineating long slender antapical horns. **23.** *Brigantedinium* spp. (Sample 189-1172A-6H-4, 85–87 cm) (2); scale bar = ~15 µm. Specimen from the Quaternary; compare with *Brigantedinium*? sp. **24.** *Cerebrocysta bartonensis* (Sample 189-1172A-49X-4, 85–87 cm) (1); scale bar = ~15 µm. (Continued on next page.)

13
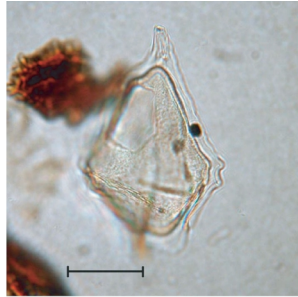
14
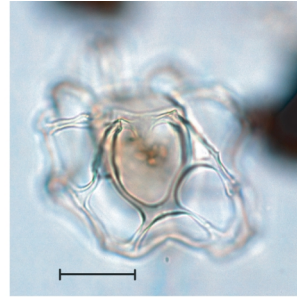
15
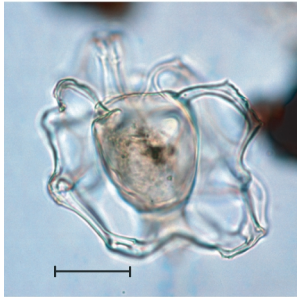
16
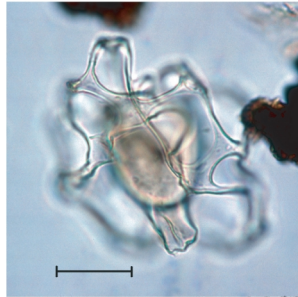
17
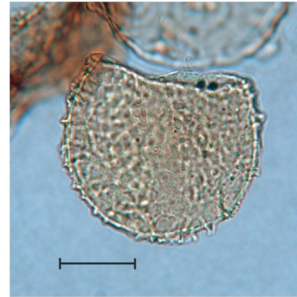
18

19

20
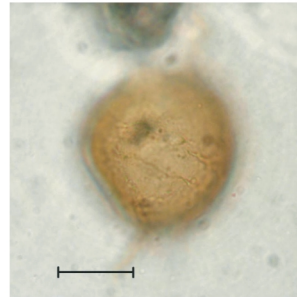
21

22
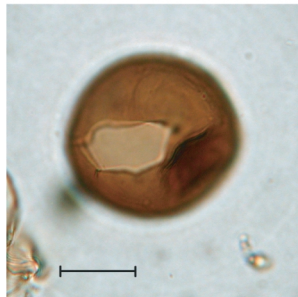
23

24

Plate P1 (continued). 25–28. *Cerodinium* sp. A; (25–27) Sample 189-1172D-24R-5, 67–69 cm (2); note elongated endocyst and short antapical horns; (28) Sample 189-1172D-24R-5, 130–133 cm (1); this specimen is somewhat comparable to *Cerodinium diebelii,* but lacks the longer antapical horns typical for that species. **29.** *Cerodinium dartmooria* (Sample 189-1172D-19R-3, 40–42) cm (1). **30, 31.** *Cerodinium speciosum;* (30) Sample 189-1172D-20R-7, 40–42 cm (1); (31) Sample 189-1172D-21R-3, 40–42 cm (1). **32, 33.** *Cerodinium striatum* (Sample 189-1172D-24R-5, 36–38 cm) (1). **34, 35.** *Charlesdowniea edwardsii* group (Sample 189-1172D-11R-5, 40–42 cm) (1). **36.** *Cleistosphaeridium diversispinosum* (Sample 189-1172D-14R-1, 40–42 cm) (2). (Continued on next page.)

25

26

27
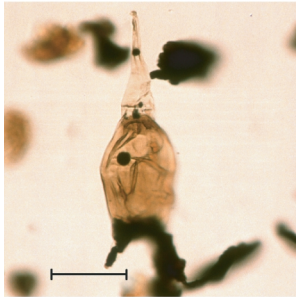
28
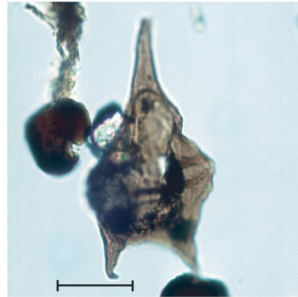
29
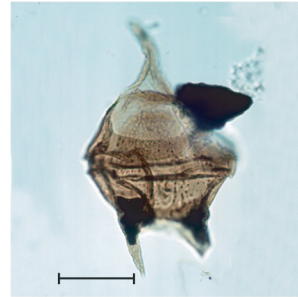
30

31

32

33
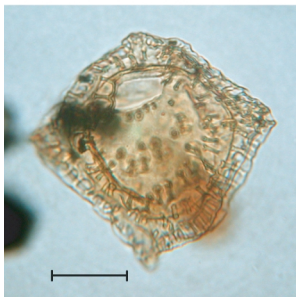
34
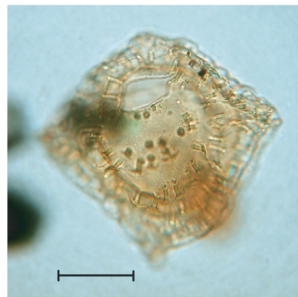
35
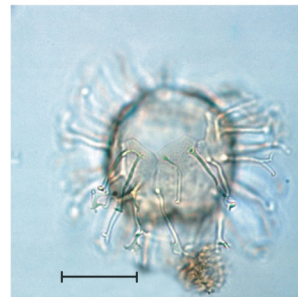
36

Plate P1 (continued). 37–39. *Cleistosphaeridium placacanthum* (Sample 189-1172D-8R-6, 40–42 cm) (2). **40–42.** *Cordosphaeridium fibrospinosum* group (Sample 189-1172D-5R-1, 40–42 cm) (1). **43.** *Corrudinium* sp. Goodman and Ford, 1983 (Sample 189-1172A-39X-5, 85–87 cm) (1). **44–47.** *Cribroperidinium* sp. A; (44, 45) Sample 189-1172A-46X-2, 85–87 cm (1); (46, 47) Sample 189-1172D-12R-1, 40–42 cm (1). **48.** *Cribroperidinium* sp. A (Sample 189-1172D-12R-1, 40–42 cm) (1). (Continued on next page.)
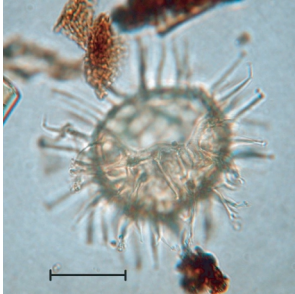
37

38

39

40

41
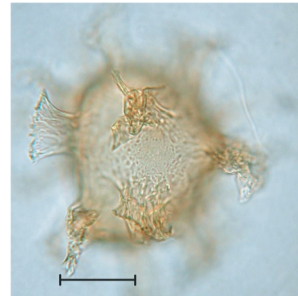
42

43

44

45

46

47

48

Plate P1 (continued). 49–52. *Deflandrea antarctica* group; (49) Sample 189-1172A-39X-6, 85–87 cm (1); (50) Sample 189-1172A-52X-5, 85–87 cm (1); (51, 52) Sample 189-1172D-3R-1, 40–42 cm (1). **53–59.** *Deflandrea convexa* group; (53) Sample 189-1172D-5R-1, 40–42 cm (1); (54, 55). Sample 189-1172D-5R-1, 40–42 cm (2); (56, 57) Sample 189-1172D-5R-1, 40–42 cm (1); (58, 59) Sample 189-1172D-8R-6, 40–42 cm (1). **60.** *Deflandrea phosphoritica* group (Sample 189-1172A-39X-4, 10–12 cm) (1). (Continued on next page.)

49
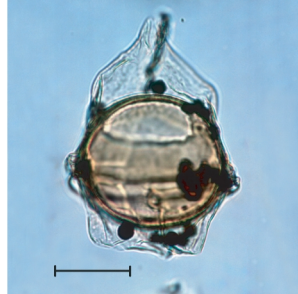
50

51

52

53

54

55

56

57

58

59

60

Plate P1 (continued). 61–63. *Deflandrea* sp. A; (61) Sample 189-1172A-39X-4, 74–76 cm (1); note triangular endophragm; (62) Sample 189-1172A-39X-4, 74–76 cm) (2); (63) Sample 189-1172A-39X-4, 74–76 cm) (1). **64, 65.** *Dinopterygium* sp. A (Sample 189-1172D-24R-5, 130–133 cm) (1). **66.** *Dracodinium waipawaense* (Sample 189-1172D-13R-2, 40–42 cm) (1). **67–69.** *Enneadocysta partridgei;* (67) Sample 189-1172A-39X-5, 105–107 cm (1); (68, 69) Short processes (*Areosphaeridium ebdonii*-style) (Sample 189-1172A-40X-2, 70–72 cm) (1); such variations are considered environmentally controlled. **70.** *Eocladopyxis peniculata* (Sample 189-1172A-48X-4, 108–110 cm (1). **71, 72.** *Glaphyrocysta* spp. (Core 189-1172D-22R). (Continued on next page.)

61
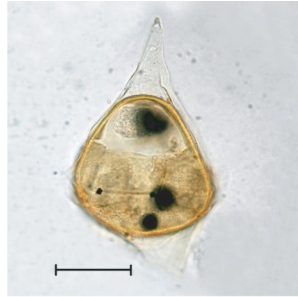
62
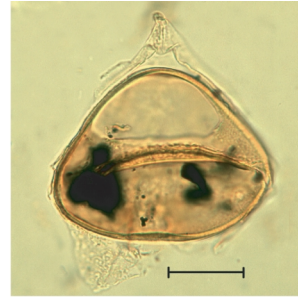
63
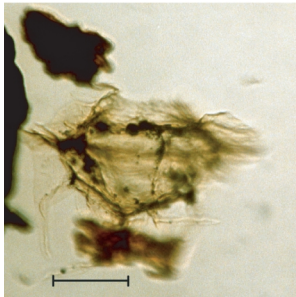
64
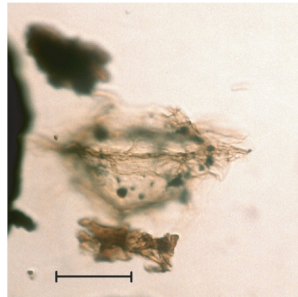
65
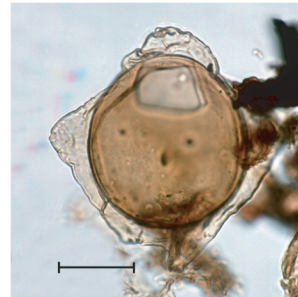
66
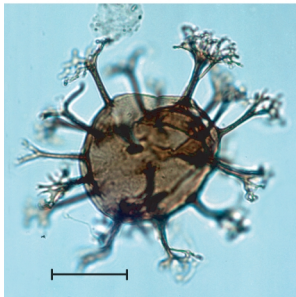
67
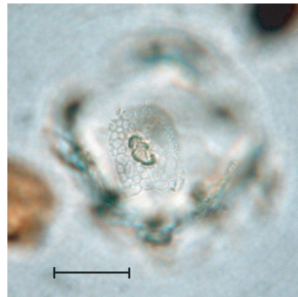
68

69
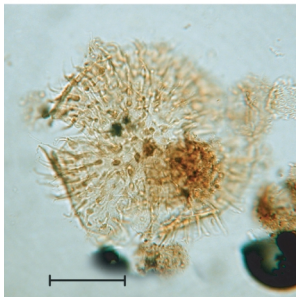
70

71
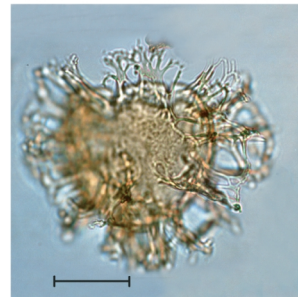
72

Plate P1 (continued). 73. *Glaphyrocysta* spp. (Core 189-1172D-22R). **74.** *Histiocysta* sp. (Sample 189-1172A-46X-2, 85–87 cm) (1). **75, 76.** *Homotryblium tenuispinosum* (Sample 189-1172A-40X-2, 70–72 cm) (1). **77.** *Hystrichokolpoma rigaudiae,* 189-1172D-11R-5, 40–42 cm (1). **78–83.** *Hystrichokolpoma truncatum* (78) Sample 189-1172A-54X-8, 85–87 cm) (1); scale bar = ~15 µm; (79, 80) Sample 189-1172D-11R-5, 40–42 cm (1); scale bar = ~15 µm; **81–83.** Sample 189-1172D-5R-1, 40–42 cm (1); scale bar = ~15 µm. **84.** *Hystrichosphaeridium truswelliae* (Sample 189-1172D-16R-2, 40–42 cm) (1).
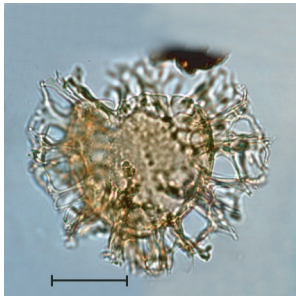
73

74
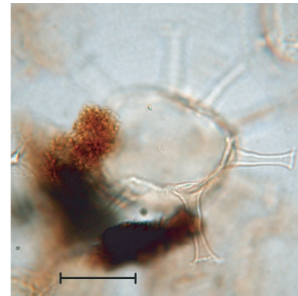
75

76

77
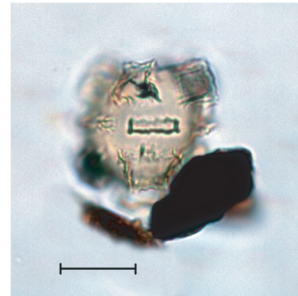
78

79

80

81

82

83
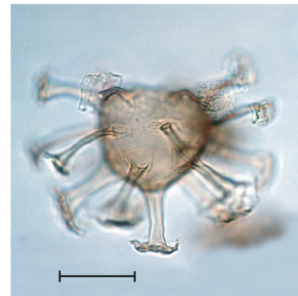
84

Plate P1 (continued). 85–87. *Hystrichosphaeridium truswelliae* (Sample 189-1172D-20R-5, 40–43 cm) (1). **88, 89.** *Hystrichosphaeridium tubiferum* (Sample 189-1172D-20-5, 40–43 cm) (1). **90, 91.** *Hystrichosphaeropsis* sp. (Sample 189-1172D-16R-2, 40–42 cm) (1). **92, 93.** *Impagidinium cassiculum* (Sample 189-1172D-14R-1, 40–42 cm) (1). **94, 95.** *Impagidinium dispertitum* (Sample 189-1172D-8R-6, 40–42 cm) (1). **96.** *Impagidinium maculatum* (Sample 189-1172D-14R-1, 40–42 cm) (1). (Continued on next page.)
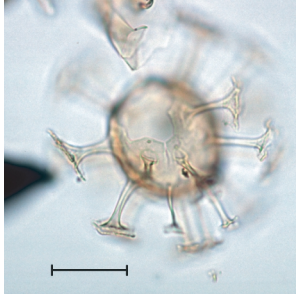
85
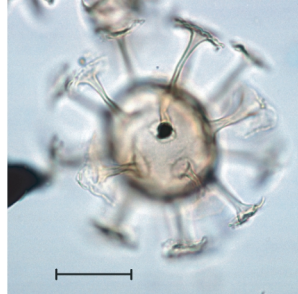
86

87

88

89
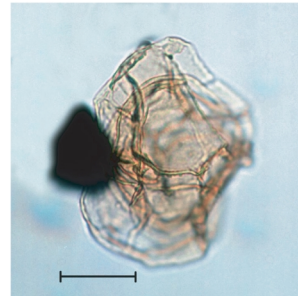
90
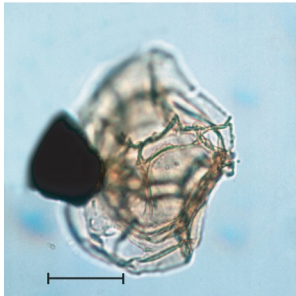
91
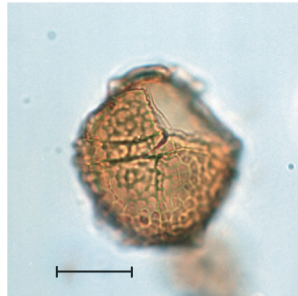
92
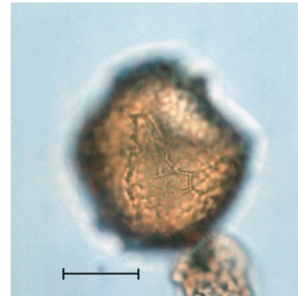
93

94

95
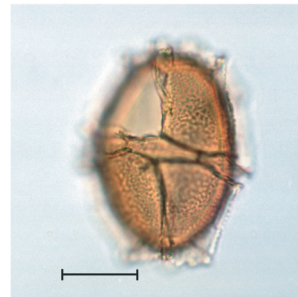
96

Plate P1 (continued). 97, 98. *Impagidinium victorianum* (Sample 189-1172A-39X-5, 105–107 cm) (1). **99.** *Lejeunecysta* sp. (Sample 189-1172A-39X-6, 55–57 cm) (1). **100–104.** *Manumiella druggii;* (100, 101) Sample 189-1172D-24R-5, 130–133 cm (1); (102–104) Sample 189-1172D-24R-5, 73–75 cm (1). **105, 106.** *Membranophoridium perforatum;* (105) Sample 189-1172D-12R-3, 85–87 cm (1); (106) Sample 189-1172D-12R-7, 40–42 cm (1). **107, 108.** *Octodinium askiniae* (Sample 189-1172A-39X-6, 105–107 cm) (1). (Continued on next page.)
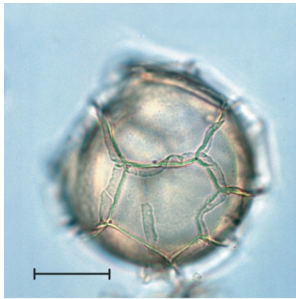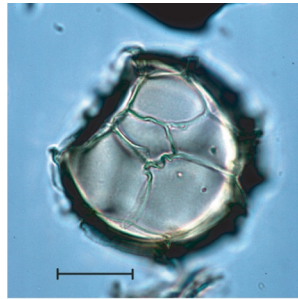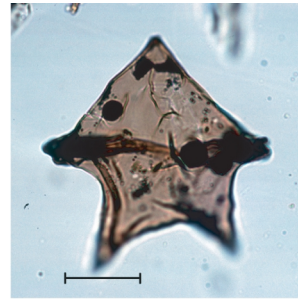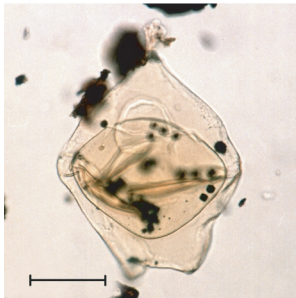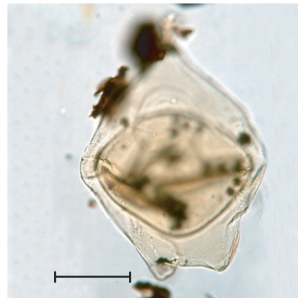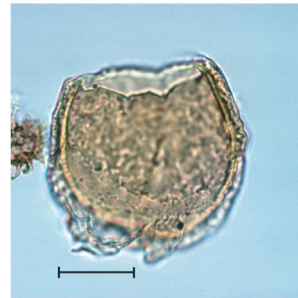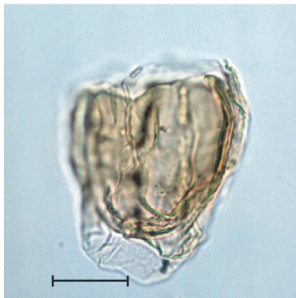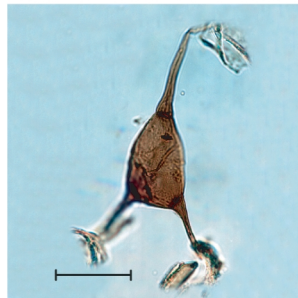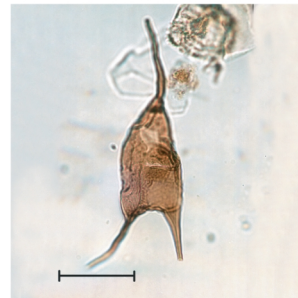
Plate P1 (continued). 109, 110. *Operculodinium?* sp. A (Sample 189-1172D-24R-5, 130–133 cm) (1); scale bar = ~15 µm; see also SEM imagery. **111, 112.** *Palaeocystodinium* sp. (Sample 189-1172D-24R-5, 30–32 cm) (1); (111) scale bar = ~30 µm; (112) close to *Andalusiella*. **113–116.** *Palaeoperidinium pyrophorum* (Sample 189-1172D-24R-5, 36–38 cm) (1). **117.** *Paucisphaeridium* sp. (Sample 189-1172A-39X-4, 14–16 cm) (1); scale bar = ~10 µm. **118, 119.** *Schematophora obscura* (Sample 189-1172D-13R-6, 40–42 cm) (1). **120.** *Schematophora speciosa* (Sample 189-1172A-39X-5, 55–57 cm) (1); scale bar = ~15 µm. **120.** *Schematophora speciosa* (Sample 189-1172A-39X-5, 55–57 cm) (1); scale bar = ~15 µm. (Continued on next page.)
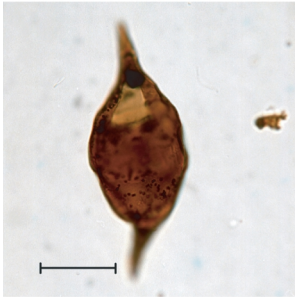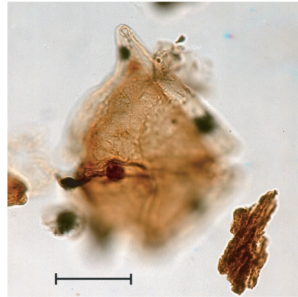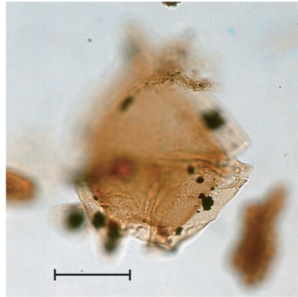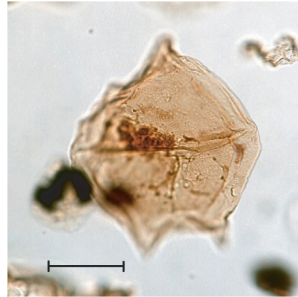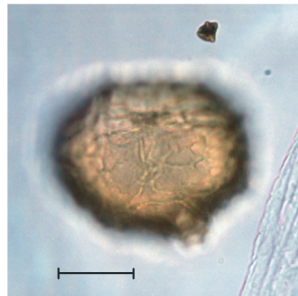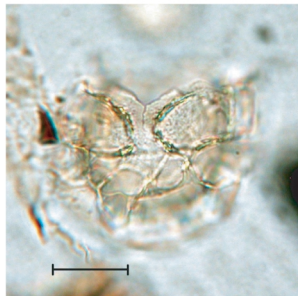
Plate P1 (continued). 121, 122. *Schematophora speciosa* (Sample 189-1172A-39X-5, 55–57 cm) (1); scale bar = ~15 µm. **123.** *Selenopemphix nephroides* (Sample 189-1172A-39X-5, 85–87 cm) (1). **124, 125.** *Senegalinium bicavatum* (Sample 189-1172D-24R-5, 30–32 cm) (1). **126–129.** *Senoniasphaera inornata* (126–128) Sample 189-1172D-24R-5, 12–14 cm (1); (129) Sample 189-1172D-24R-5, 36–38 cm (1). **130.** *Spinidinium luciae* (Sample 189-1172A-39X-5, 55–57 cm) (1). **131, 132.** *Spinidinium macmurdoense;* (131) Sample 189-1172A-39X-5, 105–107 cm (1); (132) Sample 189-1172A-39X-6, 105–107 cm (1). (Continued on next page).
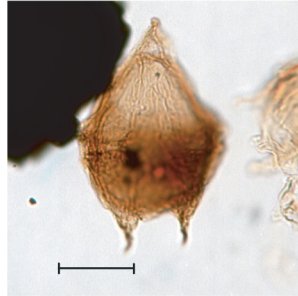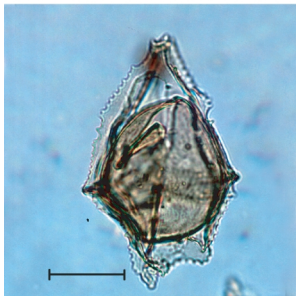
Plate P1 (continued). 133–135. *Spiniferites* sp. A (Sample 189-1172D-24R-5, 130–133 cm) (2). **136.** *Spiniferites* sp. B (Sample 189-1172A-47X-4, 85–87 cm) (1). **137, 138.** *Stoveracysta kakanuiensis* (1); (137) Sample 189-1172A-39X-3, 122–124 cm; (138) Sample 189-1172A-39X-3, 145–147 cm. **139–141.** *Trithyrodinium evittii* (Sample 189-1172D-24R-5, 12–14 cm) (1). **142.** *Turbiosphaera filosa* (Sample 189-1172A-39X-4, 10–12 cm) a (1). **143.** *Vozzhennikovia apertura* (Sample 189-1172A-39X-4, 85–87 cm) (1). **144.** *Alisocysta circumtabulata* (Sample 189-1172D-23R-1, 41–43 cm) (SEM). (Continued on next page.)
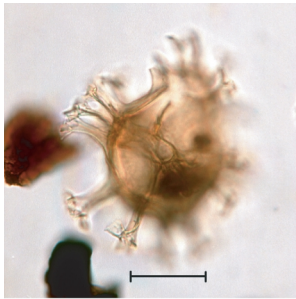
133
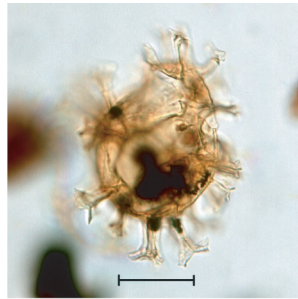
134
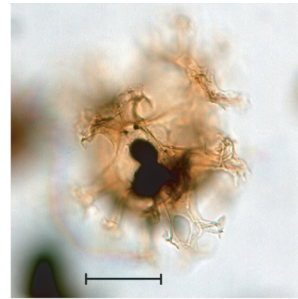
135
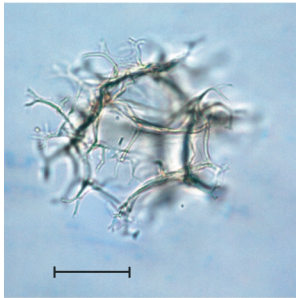
136

137
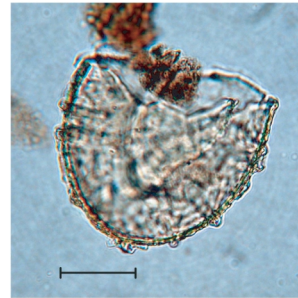
138
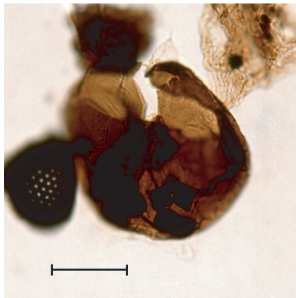
139
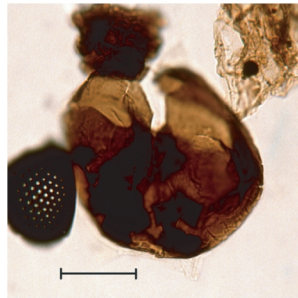
140

141
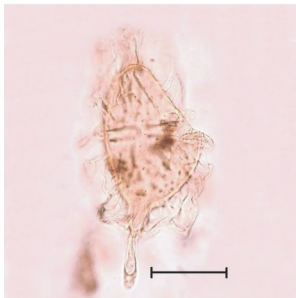
142
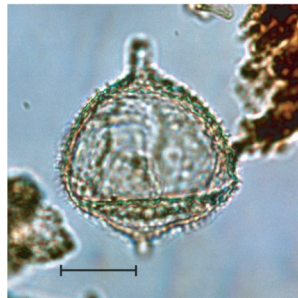
143
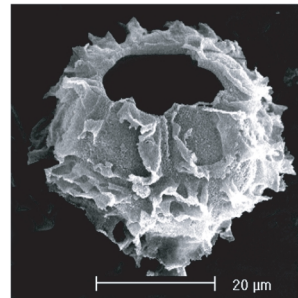
144

Plate P1 (continued). 145. *Alisocysta circumtabulata* (Sample 189-1172D-23R-1, 41–43 cm) (SEM). **146.** *Alisocysta reticulata* (Sample 189-1172D-23R-1, 41–43 cm) (SEM). **147.** *Alterbidinium* sp. (Sample 189-1172D-24R-5, 40–42 cm) (SEM). **148, 149.** *Cerebrocysta* spp. (148) Sample 189-1172D-3R-4, 40–42 cm (SEM); (149) Sample 189-1172A-39X-4, 40–42 cm (SEM). **150.** *Cerodinium dartmoorium* (Sample 189-1172D-23R-1, 41–43 cm. **151–153.** *Cerodinium* sp. A (Sample 189-1172D-29R-5, 40–42 cm) (SEM) (153: detail). **154.** *Cleistosphaeridium* spp. (Sample 189-1172D-12R-7, 40–42 cm) (SEM) **155.** *Corrudinium incompositum* (Sample 189-1172A-39X-3, 138–140 cm) (SEM). **156.** *Corrudinium* sp. Goodman and Ford, 1983 (Sample 189-1172A-39X-3, 138–140 cm) (SEM). (Continued on next page.)
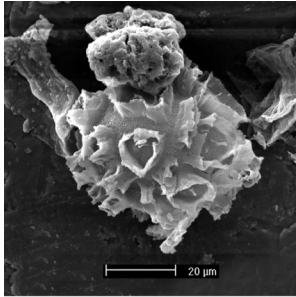
145
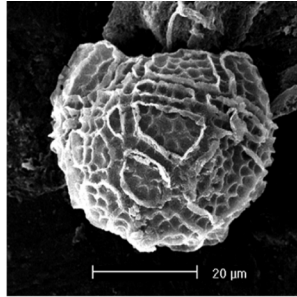
146
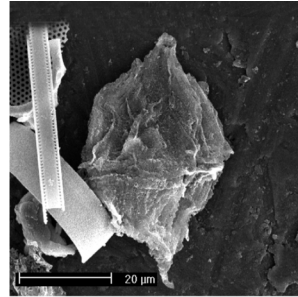
147
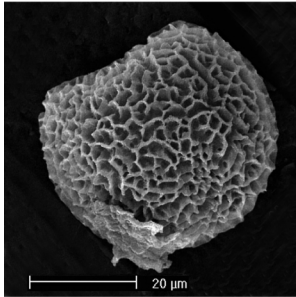
148
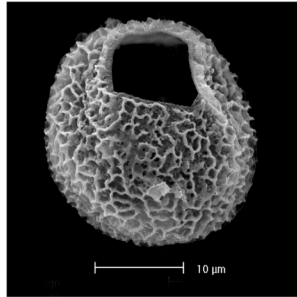
149
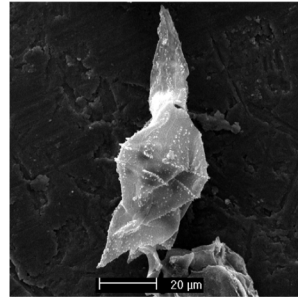
150
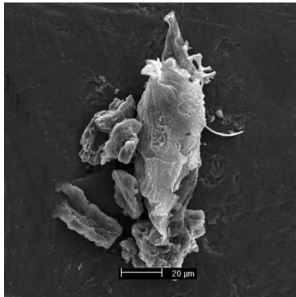
151

152
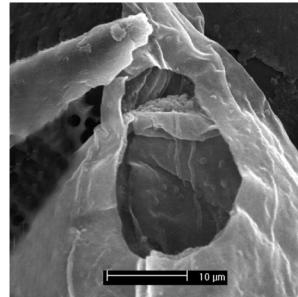
153
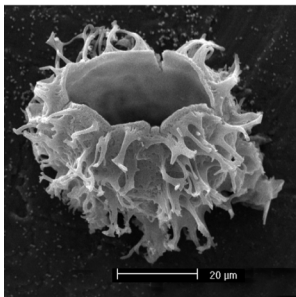
154
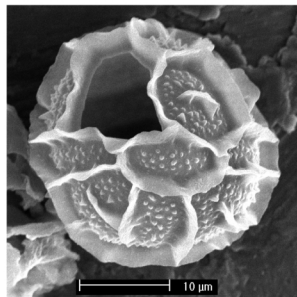
155
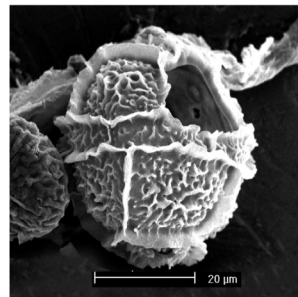
156

Plate P1 (continued). 157–160. *Deflandrea antarctica* (SEM); (157) Sample 189-1172D-12R-7, 40–42 cm; (158) Sample 189-1172D-3R-4, 40–42 cm; (159) Sample 189-1172A-39X-3, 48–50 cm; (160) Sample 189-1172A-39X-4, 147–149 cm. **161.** *Deflandrea convexa* (Sample 189-1172D-12R-7, 40–42 cm) (SEM). **162–164.** *Dinopterygium* sp. A (Sample 189-1172D-29R-5, 40–42 cm) (SEM) (162) lateral antapical view; (163) oblique apical view. **165–168.** *Dracodinium waipawaense* (Sample 189-1172D-12R-7, 40–42 cm) (SEM). (Continued on next page.)
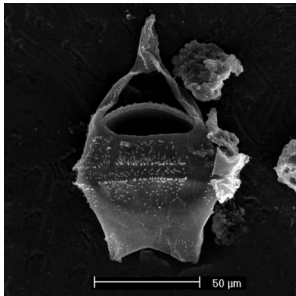
157
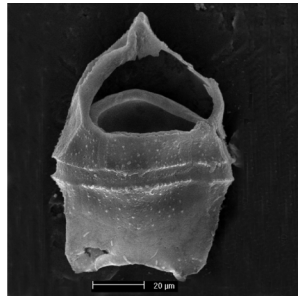
158
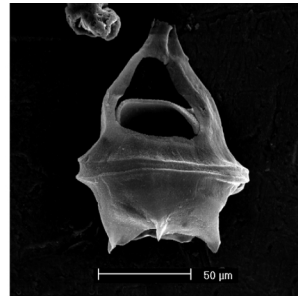
159
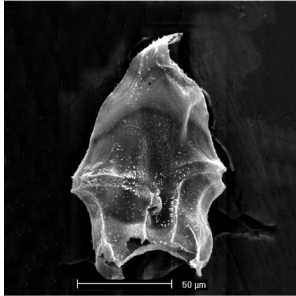
160
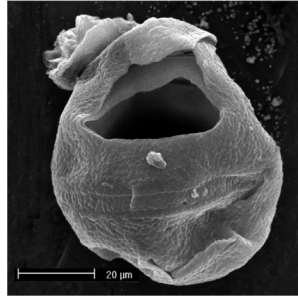
161
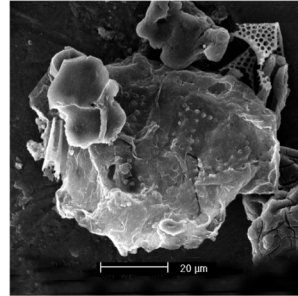
162
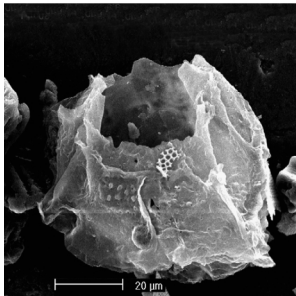
163
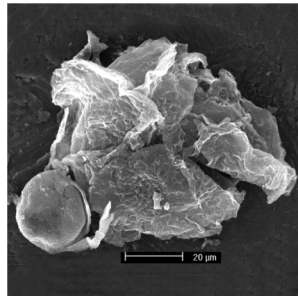
164
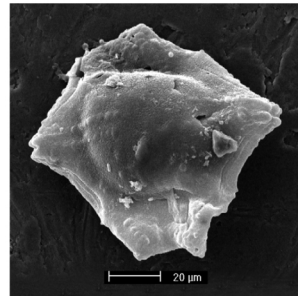
165
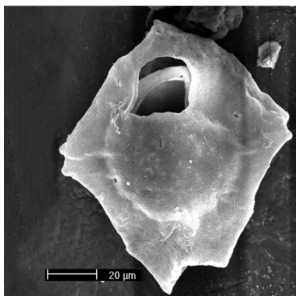
166
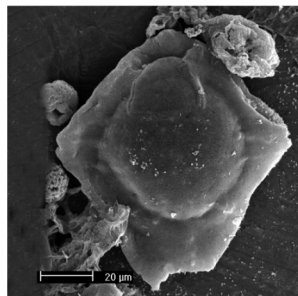
167
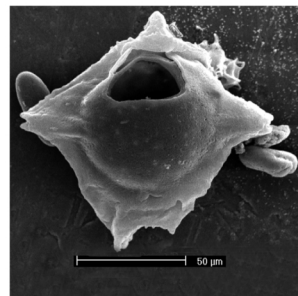
168

Plate P1 (continued). 169. *Eisenackia crassitabulata* (here part of *Alisocysta reticulata* group) (Sample 189-1172D-29R-5, 40–42 cm) (SEM). **170, 171.** *Enneadocysta* sp. A (Sample 189-1172D-3R-4, 40–42 cm) (SEM). **172.** *Enneadocysta partridgei* (Sample 189-1172A-39X-4, 147–149 cm) (SEM). **173, 174.** *Eocladopyxis* sp. (Sample 189-1172D-12R-7, 40–42 cm) (SEM); (174) note hollow processes, penetrating endophragm. **175–180.** *Glaphyrocysta* spp. (Sample 189-1172D-23R-1, 41–43 cm) (SEM); (178) detail archaeopyle margin; (180) operculum. (Continued on next page.)
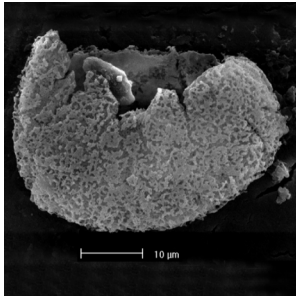
169
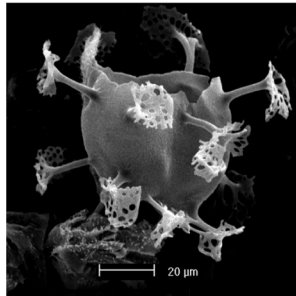
170
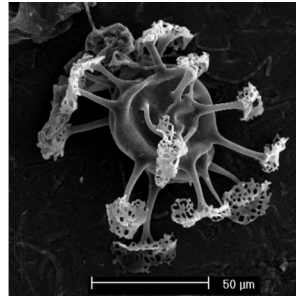
171
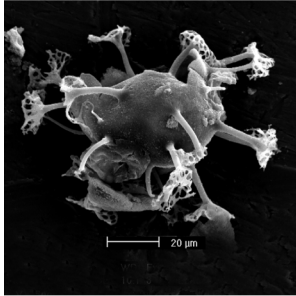
172
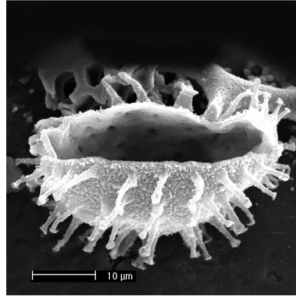
173
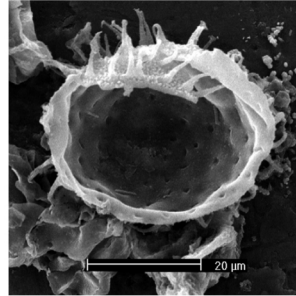
174
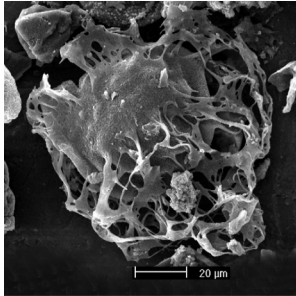
175
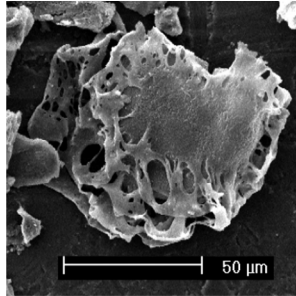
176
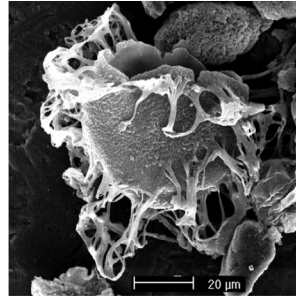
177
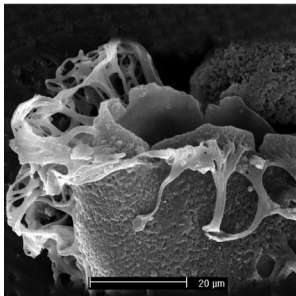
178
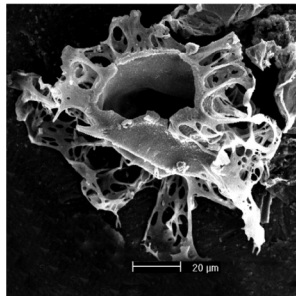
179
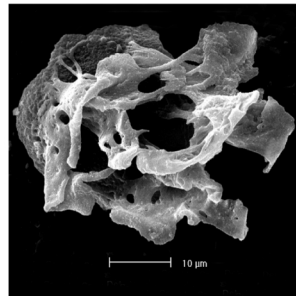
180

Plate P1 (continued). 181. *Histiocysta* sp., (possibly *Microdinium*) (Sample 189-1172D-23R-1, 41–43 cm) (SEM). **182.** *Hystrichokolpoma spinosum* (Sample 189-1172D-12R-7, 40–42 cm) (SEM). **183–185.** *Hystrichosphaeridium truswelliae* (SEM); (183) Sample 189-1172D-3R-4, 40–42 cm (operculum); (184, 185) Sample 189-1172D-23R-1, 41–43 cm; (185: detail antapical processes). **186.** *Impagidinium cassiculum* (Sample 189-1172D-12R-7, 40–42 cm) (SEM). **187.** *Impagidinium dispertitum* (Sample 189-1172A-39X-4, 147–149 cm) (SEM). **188.** *Impagidinium* spp. (Sample 189-1172D-3R-4, 40–42 cm) (SEM). **189.** *Manumiella druggii* transition to *Manumiella rotundata* (Sample 189-1172D-29R-5, 40–42 cm) (SEM). **190–192.** *Operculodinum*? sp. A (Sample 189-1172D-24R-5, 40–42 cm) (SEM). (Continued on next page.)
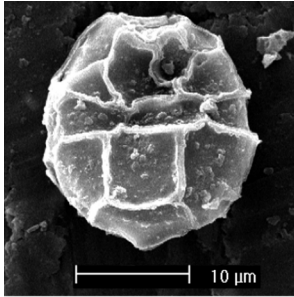
181
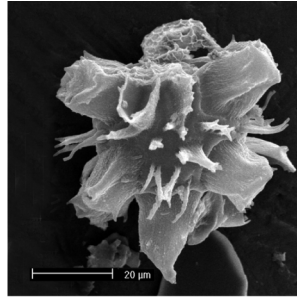
182
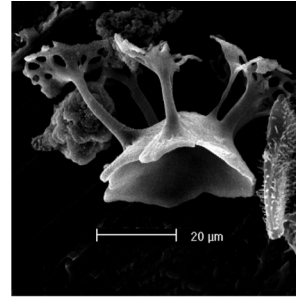
183
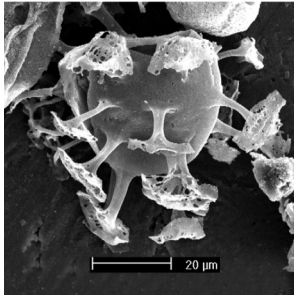
184
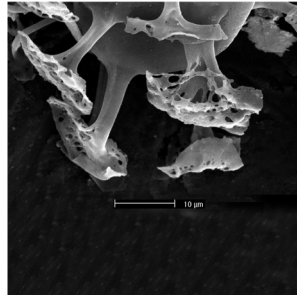
185
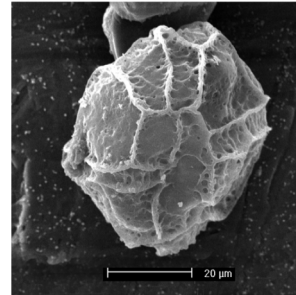
186
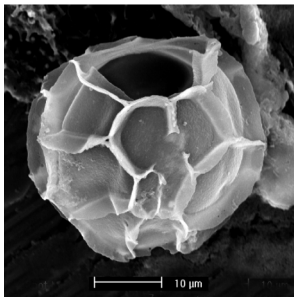
187
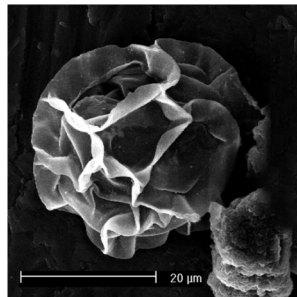
188
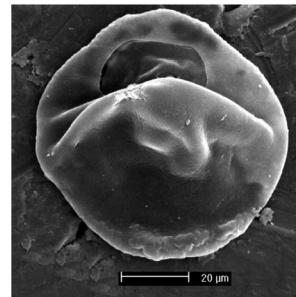
189
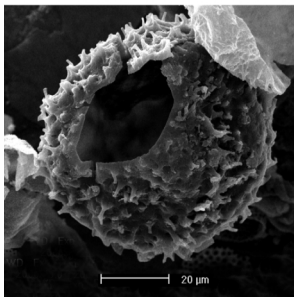
190
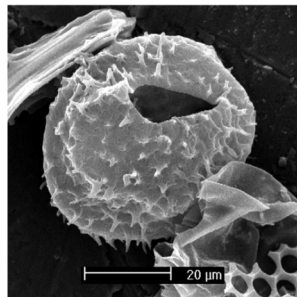
191
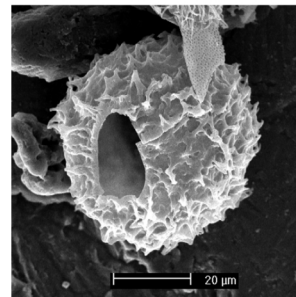
192

Plate P1 (continued). 193. *Operculodinum*? sp. A (Sample 189-1172D-24R-5, 40–42 cm) (SEM). **194–196.** *Operculodinium* spp. (SEM); (194) Sample 189-1172D-23R-1, 41–43 cm; (195, 196) Sample 189-1172A-39X-4, 147–149 cm. **197.** *Palaeocystodinium* spp. (Sample 189-1172D-23R-1, 41–43 cm) (SEM). **198–200.** *Paucisphaeridium* spp. (Sample 189-1172D-3R-4, 40–42 cm) (SEM). **201.** *Phthanoperidinium echinatum* (Sample 189-1172A-39X-3, 138–140 cm) (SEM). **202–204.** *Senegalinium dilwynense* (Sample 189-1172D-23R-1, 41–43 cm) (SEM); (202) ventral view; (203) dorsal view; (204) *Senegalinium dilwynense* (right) and *Diconodinium* sp., (left). (Continued on next page.)
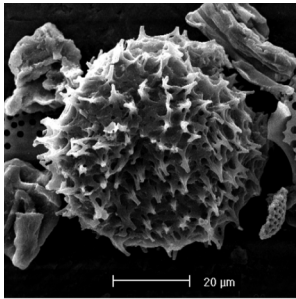
193
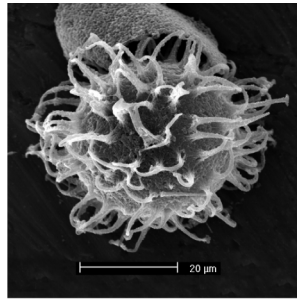
194
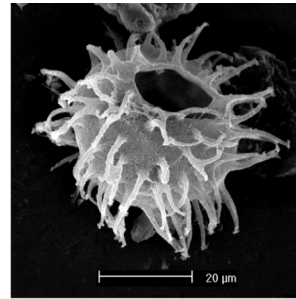
195
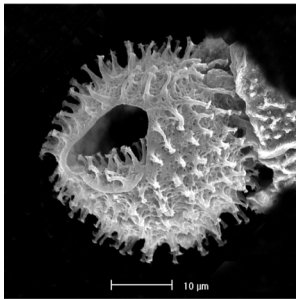
196
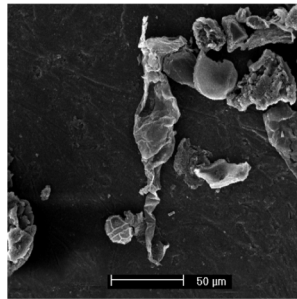
197
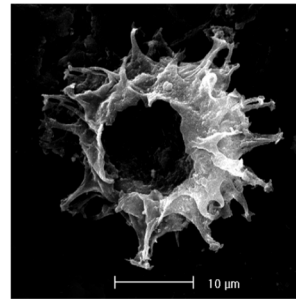
198
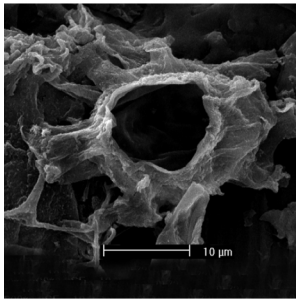
199
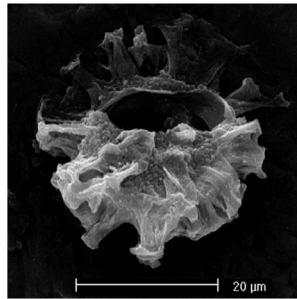
200
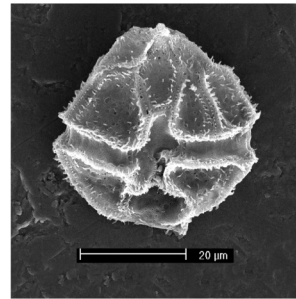
201
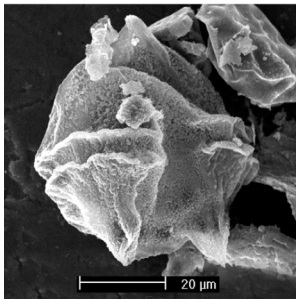
202
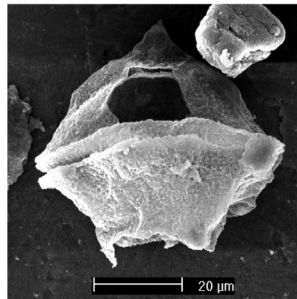
203
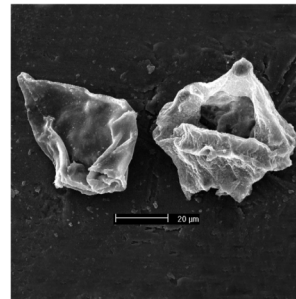
204

Plate P1 (continued). 205, 206. *Spinidinium* spp. (Sample 189-1172D-12R-7, 40–42 cm) (SEM). **207.** *Spinidinium luciae* (Sample 189-1172A-39X-6, 122–124 cm) (SEM). **208, 209.** *Spinidinium macmurdoense* (Sample 189-1172A-39X-6, 122–124 cm) (SEM). **210.** *Turbiosphaera filosa* (Sample 189-1172A-39X-3, 48–50 cm) (SEM). **211.** *Vozzhennikovia apertura* (Sample 189-1172D-3R-4, 40–42 cm) (SEM). **212.** *Vozzhennikovia?* spp. (Sample 189-1172A-39X-3, 138–140 cm) (SEM); note 3I archaeopyle. **213.** *Vozzhennikovia* spp. (Sample 189-1172A-39X-3, 138–140 cm) (SEM).
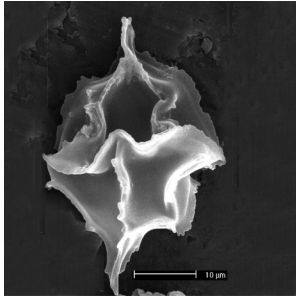
205
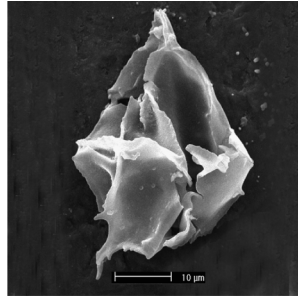
206
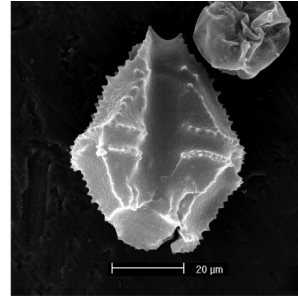
207
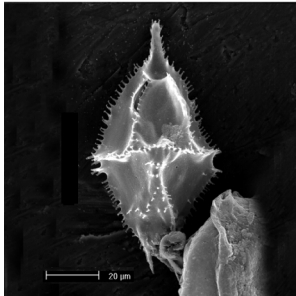
208
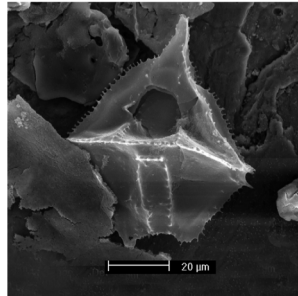
209
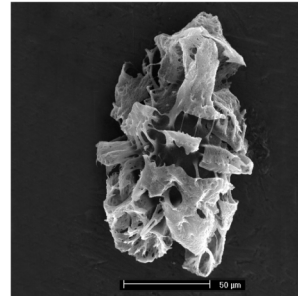
210
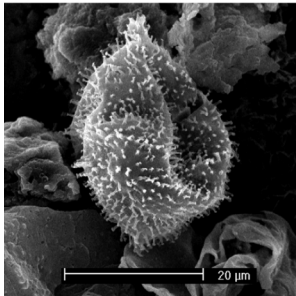
211
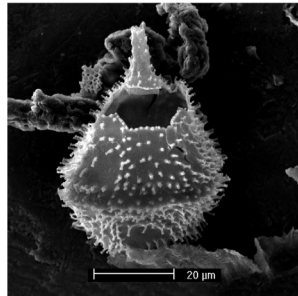
212
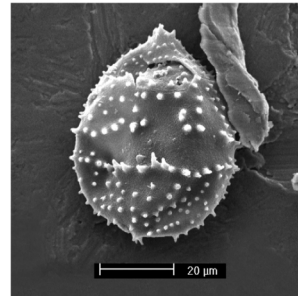
213

CHAPTER NOTES*

N1. Röhl, U., Brinkhuis, H., Stickley, C.E., Fuller, M., Schellenberg, S.A., Wefer, G., and Williams, G.L., submitted. Cyclostratigraphy of middle and late Eocene sediments from the East Tasman Plateau (Site 1172). *In* Exon, N.F., Malone, M., Kennett, J.P. (Eds.), *Cenozoic Paleoceanography and Tectonics in the Expanding Tasmanian Seaway.* Am. Geophys. Union, Geophys. Monogr.

N2. Stickley, C.E., Brinkhuis, H., Schellenberg, S.A., Sluijs, A., Fuller, M., Grauert, M., Röhl, U., Warnaar, J., and Williams, G.L., submitted. Timing and nature of the opening of the Tasmanian Gateway at the Eocene-Oligocene transition: ODP Site 1172. *In* Exon, N.F., Malone, M., and Kennett, J.P. (Eds.), *Cenozoic Paleoceanography and Tectonics in the Expanding Tasmanian Seaway.* Am. Geophys. Union, Geophys. Monogr.

N3. Röhl, U., Brinkhuis, H., and Fuller, M., submitted. On the search for the Paleocene/Eocene boundary in the Southern Ocean: exploring ODP Leg 189 Holes 1171D and 1172D, Tasman Sea. *In* Exon, N.F., Malone, M., and Kennett, J.P. (Eds.), *Cenozoic Paleoceanography and Tectonics in the Expanding Tasmanian Seaway.* Am. Geophys. Union, Geophys. Monogr.

N4. Schellenberg, S.A., Stickley, C.E., Brinkhuis, H., Fuller, M., Kyte, F., and Williams, G.L., in review. The Cretaceous–Palaeogene transition at ODP Site 1172 (East Tasman Plateau, southwestern Pacific). *In* Exon, N.F., Malone, M., and Kennett, J.P. (Eds.), *Cenozoic Paleoceanography and Tectonics in the Expanding Tasmanian Seaway.* Am. Geophys. Union, Geophys. Monogr.

N5. Huber, M., Brinkhuis, H., Stickley, C.E., Döös, K., Sluijs, A., Warnaar, J., Schellenberg, S.A., and Williams, G.L., submitted. Eocene circulation of the Southern Ocean: was Antarctica kept warm by subtropical waters? *Science.*

*Dates reflect file corrections or revisions.